

**Universidade de Lisboa
Faculdade de Farmácia**



**Development of hybrid lipidic-polymeric
nanoparticles with hyaluronic acid
encapsulating Dimethylfumarate and Rutin
by modified nanoprecipitation**

Adriana Reis Morais

Trabalho de campo orientado pela Professora Doutora Carla Serri,
Professora Auxiliar da Universidade de Sassari e Coorientado pelo
Professor Doutor António José Leitão das Neves Almeida, Professor
Catedrático da Faculdade de Farmácia da Universidade de Lisboa

Mestrado Integrado em Ciências Farmacêuticas

2023

Universidade de Lisboa
Faculdade de Farmácia



Development of hybrid lipidic-polymeric nanoparticles with hyaluronic acid encapsulating Dimethyl fumarate and Rutin

Adriana Reis Morais

Trabalho final de Mestrado Integrado em Ciências Farmacêuticas
apresentado à Universidade de Lisboa através da Faculdade de Farmácia

Trabalho de campo orientado pela Professora Doutora Carla Serri,
Professora Auxiliar da Universidade de Sassari e Coorientado pelo
Professor Doutor António José Leitão das Neves Almeida, Professor
Catedrático da Faculdade de Farmácia da Universidade de Lisboa

2023

This research project was developed under the Erasmus + Programme in the Faculty of Pharmacy of University of Sassari in Sardinia, Italy, under the guidance of professor Giovanna Rassu and Doctor Carla Serri.



Abstract

Background: Dimethylfumarate, a medication employed in multiple sclerosis, and Rutin, a bioflavonoid, are both recognized as anti-neuroinflammatory agents linked to neurodegenerative diseases. Nevertheless, they present poor solubility and a limited bioavailability. To tackle these challenges, nanotechnology has made a remarkable advancement in ameliorating such issues. Therefore, hybrid lipidic-polimeric nanoparticles have been synthesized, taking leverage of both components to enhance the therapeutic effect and facilitate the intranasal route as there is an anatomical connection between the nasal cavity and the central nervous system. **Purpose:** The aim of this study is to evaluate how different quantities of several excipients on nanoparticles impacts the physicochemical characterization of the formulation as well as to determine the most effective preparation technique. **Methods:** Modified nanoprecipitation, wherein the organic component consisted of either phosphatidylcholine or a PEGylated-lipid dissolved in ethanol, while the polymeric component is represented by hyaluronic acid dissolved in water. The first two formulations were produced only with the resource of the vortex while the remaining formulations were produced with the syringe pump method, involving the gradual dropwise addition of oil into the water. Both approaches were followed by solvent evaporation and physicochemical characterization along with entrapment efficacy. **Results:** The modified nanoprecipitation performed with the sonicator resulted in larger nanoparticles compared to those produced using the syringe pump. In general, the percentage of poloxamer, cholesterol, palmitoylethanolamide, the choice of the lipid component, and the absence of hyaluronic acid affect the particle size in the formulations. Formulation 8 may be the most suitable for intranasal delivery of dimethyl fumarate, while formulations 13 or 14 could transport rutin via the same route.

Palavras-chave: Dimethyl fumarate; Rutin; Multiple Sclerosis; Nanoparticles; Multiple Sclerosis; Intranasal route;

Resumo

Contexto: O fumarato de dimetilo, fármaco utilizado na esclerose múltipla, e a rutina, um bioflavonóide, são ambos agentes anti-neuroinflamatórios relacionados a doenças degenerativas, apresentando, porém, uma fraca solubilidade e uma limitada biodisponibilidade. Para contornar estas questões, a nanotecnologia tem feito avanços notáveis na melhoria de tais problemas. Assim, nanopartículas híbridas lipídico-poliméricas foram sintetizadas, aproveitando o benefício de ambos os componentes para melhorar o efeito terapêutico e facilitar a administração por via intranasal, uma vez que existe uma ligação anatômica entre a cavidade nasal e o sistema nervoso central. **Objetivo:** O propósito deste estudo é avaliar como diferentes quantidades de diversos excipientes na formulação afetam a caracterização físico-química, bem como determinar a técnica de preparação mais eficaz. **Métodos:** Nanoprecipitação modificada, em que o componente orgânico consiste em fosfatidilcolina ou num lípido peguado dissolvido em etanol, enquanto o componente polimérico é representado pelo ácido hialurônico dissolvido em água. As duas primeiras formulações foram produzidas apenas com o recurso ao sonicador, enquanto as restantes formulações foram produzidas com o método da bomba de seringa de perfusão, envolvendo a adição gradual de gota a gota de óleo na água. Ambas as abordagens foram seguidas de evaporação do solvente e caracterização físico-química, juntamente com a eficácia do aprisionamento das substâncias ativas. **Resultados:** A nanoprecipitação modificada feita com o sonicador produziu nanopartículas maiores do que as feitas com o auxílio da bomba de seringa de infusão e a distribuição de tamanho foi heterogênea na maior parte das formulações. Em geral, a percentagem de poloxâmero, colesterol, palmitoiletanolamida, a escolha do componente lipídico e a ausência de ácido hialurônico afetam o tamanho das partículas das formulações. A formulação de 8 poderá ser a mais adequada para a administração intranasal de fumarato de dimetilo, enquanto as formulações 13 ou 14 poderiam transportar rutina pela mesma via.

Palavras-chave: Fumarato de dimetilo; Rutina; Esclerose Múltipla; Nanopartículas; Via intranasal;

Acknowledgements

First thing first, I would like to thank professor Giovanna Rassu for accepting me into her department and giving me good knowledge about this topic. To Professor Carla Serri I am very grateful for having you as my supervisor. You taught me a lot, helped me and gave me feedback to this study that would not be done without you. To professor António Almeida, I am also really thankful for accepting me and for all the feedback you have given me. Thank you for trusting me and guiding me.

Secondly, I want to thank my forever lab partner and friend, Alessia Canu, who made laboratory days so fun. Those four months in Sassari would not be the same without you and your helpful quality was very appreciated. From assessing the particle sizes to having our tea break, I will always cherish our good memories within.

To my mom, that always supported me and was there for me to hold me and reassuring everything would be alright when I was having a bad moment, thank you for everything you do for me. “A entrada na escolinha foi comigo.” That was a sentence my mother wrote on my academic ribbon. And know, the conclusion of it is with her too.

To my grandma, my dad, my brother and my family that were always helping me emotionally on the most difficult moments, I want to thank them as well.

To my friends, some who were here during the beginning of this journey, others that appeared later, thank you for all the moments we have shared together. I am grateful for all of you.

Thank you very much.

Abbreviations

API	Active Pharmaceutical Ingredient
AR	Adverse Reactions
BBB	Blood Brain Barrier
BCS	Biopharmaceutical Classification System
CDDS	Colloidal Drug Delivery Systems
CNS	Central Nervous System
CSF	Cerebrospinal fluid
DL	Drug loading capacity
DMF	Dimethyl fumarate
DMT	Disease Modifying Therapies
EE	Entrapment efficacy
EMA	European Medicine Agency
ECM	Extracellular Matrix
EtOH	Ethanol
FDA	Food and Drug Administration
GlcA	Glucuronic Acid
GlcNAc	N-acetyl-d-glucosamine
HA	Hyaluronic Acid
HAS	Hyaluronic Acid Synthetase
HLA	Human Leukocyte Antigen
HMW-HA	High molecular weight-Hyaluronic Acid
HPLC	High Performance Liquid Chromatography
IFNβ	Interferon- β
LCPS	Lipidic-core polymeric-shell

LPHNP	Lipid-polymeric Hybrid Nanoparticle
MHC	Major Histocompatibility Complex
MS	Multiple Sclerosis
MSIF	Multiple Sclerosis International Federation
NP	Nanoparticles
PI	Polydispersity Index
PLGA	Poly(Lactic-co-Glycolic Acid)
RRMS	Relapsing-Remitting Multiple Sclerosis
SD	Standard deviation

Index:

1	Introduction.....	11
1.1	Multiple Sclerosis	11
1.1.1	Pathology	11
1.1.2	Etiology.....	11
1.1.3	Treatment	12
1.1.4	Dimethyl fumarate	13
1.2	Alternative treatments for inflammatory disease – The flavonoids.....	14
1.2.1	- Rutin	15
1.3	Nose-to-brain Delivery	15
1.3.1	Blood Brain Barrier.....	16
1.3.3	Nasal Anatomy.....	18
1.3.3.1	Intracellular pathway	19
1.3.3.2	Extracellular pathway	19
1.3.4	Nanoparticles in Nose-to-brain delivery	20
1.4	Colloidal drug delivery systems.....	22
1.4.1	Nanoparticles	22
1.4.1.1	Polymeric Nanoparticles	23
1.4.1.2	Liposomes	23
1.4.1.3	Lipid-Polymer Hybrid nanoparticles (LPHNP).....	23
1.4.1.4	Composition of LPHNP.....	25
1.4.2	Methods for LPHNPs preparation	25
1.4.2.1	Modified Nanoprecipitation: Sonication.....	26
1.4.2.2	Modified Nanoprecipitation: Syringe Pump Method	27
1.4.2.3	Excipients of formulations	27
1.5	Hyaluronic acid.....	28
1.5.1	. Composition.....	28
1.5.2	Hyaluronic Acid as medicine carrier	29
2	Aim of Study.....	31
3	Materials and Methods.....	32
3.1	Materials	32
3.1.1	General Materials.....	32
3.1.2	KD Scientific Single Syringe Infusion Pump.....	32
3.1.3	Chemicals.....	35
3.2	Methods.....	36
3.2.1	Preparation of LPHNP	36
3.2.1.1	Water phase preparation	36
3.2.1.2	Organic phase preparation	37
3.2.1.3	Modified Nanoprecipitation: Sonication.....	38
3.2.1.4	Modified Nanoprecipitation: Syringe Pump method.....	38
3.2.1.5	Solvent evaporation	38
3.2.2	Physicochemical characterization of the nanoparticles	39
3.2.2.1	Particle Size	39
3.2.2.2	Polydispersity Index.....	39
3.2.2.3	Stability over time.....	40
3.2.3	Drug loading of the API.....	40
3.2.3.1	Drug loading of DMF	40
3.2.3.2	Drug loading of Rutin	41
4	Results and Discussion	42
4.1	Particle size and Polydispersity Index	42

4.1.1 Modified Nanoprecipitation: Sonication.....	42
4.1.3 Modified Nanoprecipitation: Syringe Pump Method	44
4.1.4 Stability over time.....	45
4.2 Drug Loading of the API	55
4.2.1. Drug loading of DMF	55
4.2.2 Drug loading of Rutin	56
5 Conclusion	57
6 References.....	58

Table Index:

Table 1: Components of the water and organic phase.	35
Table 2: Chemicals used for the loading analysis of the API.	36
Table 3: Percentages of components and methodology of LCPS-1 to LCPS-15.....	37
Table 4: Mean diameter and mean polydispersity Index size of nanoparticles prepared by modified nanoprecipitation: sonication.....	44
Table 5: Mean diameter and mean polydispersity Index size of nanoparticles prepared by modified nanoprecipitation: syringe pump technique.....	45
Table 6: Drug loading of dimethyl fumarate within LCPS-7 and LCPS-8.	55
Table 7: Drug loading of dimethyl fumarate within LCPS-13 and LCPS-14.....	56

Figure Index:

Figure 1: DMF molecular structure. Adapted by (13). 14

Figure 2: Molecular structure of Rutin. Adapted from (19). 15

Figure 3: Schematic diagram for different mechanisms for BBB crossing. Adapted from (20). 17

Figure 4: Schematic diagram of BBB structure. Adapted from (20). 18

Figure 5: Direct nose-to-brain routes. Adapted from (29). **A)** Respiratory pathway: the intracellular medicine transport can occur in this region by the trigeminal nerve located both in the respiratory as well as in the olfactory region. **B)** The olfactory pathway com comprehends the intracellular pathway (transcellular and through the olfactory nerves) and the extracellular/paracellular pathway between epithelial cells. 20

Figure 6: Lipidic-core polymeric-shell nanoparticle. Adapted from (47). 25

Figure 7: Molecular structure of Hyaluronic Acid. Adapted from (64). 29

Figure 8: Schematic picture of the KDS 100 Model Scientific Single Syringe Infusion Pump. Adapted from (70). 34

Figure 9: Diagram of nanoparticle's scheme. 39

Figure 10: Physicochemical stability of LCPS-1 and LCPS-2, both formulations done with the resource of the sonicator. 46

Figure 11: Physicochemical stability of LCPS-5 and LCPS-6, made with the resource of the syringe pump method. 47

Figure 12: Physicochemical stability of LCPS-3, LCPS-8 and LCPS-11 made with the resource of the syringe pump. 49

Figure 13: Physicochemical stability of LCPS-9 made with the resource of the syringe pump technique. 49

Figure 14: Physicochemical stability of LCPS-10 made with the resource of the syringe pump technique. 49

Figure 15: Physicochemical stability of LCPS-8 and LCPS-11 made with the resource of the syringe pump technique. These formulations do not contain HA. 50

Figure 16: Physicochemical stability of LCPS-14 made with the resource of the syringe pump technique. This formulation does not contain HA. 51

Figure 17: Physicochemical stability of LCPS-7, LCPS-8 and LCPS-15, made with the resource of the syringe pump. These formulations contain dimethyl fumarate. 53

Figure 18: Physicochemical stability of LCPS-13 and LCPS-14 made with the resource of the syringe pump, both containing rutin. 54

1 Introduction

1.1 Multiple Sclerosis

Neurodegenerative diseases are increasing globally, with socioeconomic burdens associated, according to healthcare statistics. In conformity with the World Health Organization, neurological disorders have been reported as the third cause of mortality worldwide (1).

The most common non-traumatic disease in young people is multiple sclerosis, affecting people between 20 to 40 years of age (2). According to MSIF (Multiple Sclerosis International Federation), it is known to affect about 2.3 million people worldwide, being more prevalent in America and Europe with a ratio of 140 cases per 100,000 and 108 per 100,000, respectively (3).

1.1.1 Pathology

Multiple Sclerosis (MS) is an auto-immune inflammatory demyelinating disease of the central nervous system (CNS) that can manifest into a heterogeneity of clinical manifestations. The pathogenesis of MS involves increased migration of activated lymphocytes across the blood-brain barrier (BBB) into the CNS, where they cause demyelination, oligodendrocyte loss, gliosis and neuro-axonal degeneration. As this inflammatory process takes place, the accumulation of focal plaques (lesions) in both white matter and grey matter occur primarily in the brain, optic nerve and spinal cord (2).

Consequentially, as the disease may affect many regions of the CNS, several systems can be affected either sensory systems or motor ones. However, the manifested clinical features will depend on the region of such lesions and on the characteristics of each individual, where the most common ones are fatigue, visual disturbances, weakness, cognitive impairment and motor disability (2,4,5).

1.1.2 Etiology

Regarding its etiology, MS occurs as a result of several factors all partaking in the disease development and it is known that the progress of the disease depends of a complex interaction between environmental, genetic and lifestyle factors (2,5).

Vitamin D deficiency, ultra-violet B light (UVB) or Epstein-Barr Virus exposure as well as smoking (mostly in men) and obesity are strong components that can cause the arising of the disease (2,5,6).

Despite of these causes, there is also a strong genetic predisposition on certain people, and the main genetic risk associated with MS resides in the major histocompatibility complex (MHC) on chromosome 6, being the human leukocyte antigen (HLA) region the most important. Most autoimmune diseases have been associated with such region however in MS, carriers of the HLA-DRB1*15 allele are considerably susceptible to develop MS 3 times more than non-carriers (7). Hence, the HLA locus is responsible for around 20-30% of susceptibility in MS (8).

About 85% of patients with MS are diagnosed with a relapsing-remitting multiple sclerosis (RRMS), the most common disease course. The gender ratio of men and women with this condition is 1:3 and its diagnosis is made primarily in the 20s and 30s. It is characterized by clearly defined relapses or exacerbations of neurologic symptoms that can endure 24 hours and are followed by periods of partial or complete remission (5).

However, usually in about 10 years in, such stage can transition to a secondary progressive disease course that can worsen neurological function or accumulate disability over time (2,5).

Therefore, it is important to manage the relapses of the disease and to prevent its progression, whether it be resorting to pharmacological or non-pharmacological approaches.

1.1.3 Treatment

Although MS presents no cure, at least to this day, several medicines are approved by EMA (European Medicine Agency) and the FDA (Food and Drug Administration) to target the neuroinflammation and the neurodegeneration of the disease, the so-called disease modifying therapies (DMT). Their function is to treat exacerbations, manage the symptoms and to modify the disease's natural course (5,9).

The first FDA approved medicine for MS was interferon- β (IFN β) in 1993 because of its anti-viral properties (10). Subsequently, other injectable molecules were approved for the treatment of the disease such as glatiramer acetate as first-line therapy and

natalizumab and mitoxantrone as a second-line therapy (5). However, the demand of an intramuscular or subcutaneous injection enables for the decrease of the patient's adherence to the treatment (2,5). Another aspect to consider is that despite their security, these pharmaceuticals can lead to injection-related adverse effects (ARs), liver dysfunction and development of neutralizing antibodies risking the effectiveness. Although there is a 30% decrease of relapse rate, this percentage is still not enough and better molecules are needed (11).

1.1.4 Dimethyl fumarate

Over the last two decades, revolutionary developments have been done in order to discover new molecules and potential therapeutic molecules for the pathology, being the oral DMT approved to enhance the patient's compliance of the treatment and being able to treat RRMS (2,5,11).

The current medicines are fingolimod, teriflunomide, and dimethyl fumarate (DMF), however the focus of this dissertation will be the latter substance. Figure 1 represents an illustration of the molecular structure of dimethyl fumarate.

The main mechanism of action of this pharmaceutical is still not well known, nonetheless, regarding the context of MS, it is believed to reduce lymphocyte counts and the disruption of cell migration (11). The anti-inflammatory and cytoprotective properties emerge from the activation of the nuclear factor (erythroid-derived 2)-like 2 transcriptional pathway, which is involved in the cellular response to oxidative stress (5).

The downregulation of the transmigration of cells across the blood-brain-barrier by reducing the endothelium adhesion is also another believed treatment-phenomenon associated with DMF (2,11).

Regarding the biopharmaceutical classification system (BCS), the molecule has not been well determined as it can belong to the class I type, meaning that such molecule is highly soluble and highly permeable (12). However, a more recent update has been done as according to the European Medicines Agency, "*the active substance is a non-hygroscopic, white to off-white powder, practically insoluble in water at 15-25°C and highly soluble in aqueous media over the pH range of 1.2-6.8 at 37±1°C according to BCS system*" (13), which is rather controversial. Therefore, solubility and permeability issues may occur.

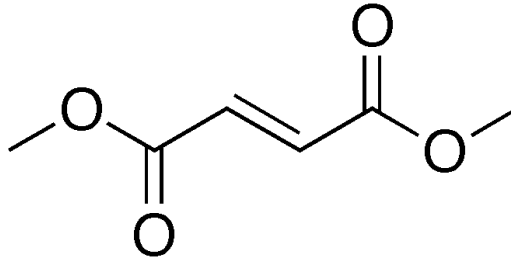


Figure 1: DMF molecular structure. Adapted by (13).

1.2 Alternative treatments for inflammatory disease – The flavonoids

Multiple sclerosis follows a neuroinflammatory course that enables oligodendrocyte damage and demyelination. In the early stages of MS, axons are relatively preserved, however, as disease progresses, an irreversible axonal damage development takes place and the RRMS is the predominant stage where a deeper lymphocytic inflammation occurs (6).

Therefore, to delay the inflammatory processes and the clinical manifestations to develop in a rapid pace, studies have shown that a healthy and active lifestyle, with fruits and vegetables included can help provide nutrients that add value to the anti-inflammatory properties (14).

Within the natural, plant-based nutrients mentioned with such characteristics are flavonoids. Flavonoids are a group of polyphenolic plant compounds that possess many health benefits in several cell systems and depending on its characteristics they can be divided into 6 subclasses (15). However, for the matter of this dissertation, flavonols will be the highlighted class.

It is known that flavonoids, being the immunomodulatory molecules that they are, can reduce demyelination and reduce the immune system excessive response (15).

In regards of MS, flavonols have shown to be able to decrease the amount of myelin phagocytosed by macrophages as well as controlling the immune response via IL-1 and TNF- α , delaying T-cell activation and demyelination, respectively (15).

Besides mentioned processes, flavonoids are also natural anti-oxidative substances as well as possessing the ability to modulate numerous cell signaling pathways as they

can interact with multiple sites at the brain tissue, showcasing neuroprotective effects (15).

1.2.1 - Rutin

Rutin, also known as Vitamin P, is a lipophilic flavonoid widely distributed in plants that has a potential effect to prevent cerebral ischemia (16). Due to its therapeutic and nutritional properties, rutin became one of the most popular bioflavonoids consumed worldwide (17). Figure 2 illustrates rutin's molecular structure.

However, as a weak acid the solubility of the bioflavonoid in water is low, which can difficult the delivery of the molecule in the organism resulting in less bioavailability, degradation and possible first-pass hepatic metabolism, not to mention the limitations associated with the BBB (16,18).

In other hand, the solubility in polar solvents like alcohols and ethanol is very high due to its polar nature (17).

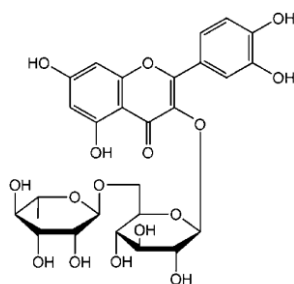


Figure 2: Molecular structure of Rutin. Adapted from (19).

1.3 Nose-to-brain Delivery

It is highly strenuous to deliver medicine to the brain due to the BBB. Thus, a plethora of developed delivery strategies regarding the brain are being developed such as convection enhanced delivery, intracranial implantation and deep-brain stimulation (20).

Other approaches are also in development, for example, intra-cerebrovascular, intra-cranial and intra-parenchymal injections (21). Unfortunately, these procedures are very risky and invasive to the patient as they may rely on surgical interventions. The brain exposure these methods consist of and the damage they may cause make them very difficult to achieve long-term usage (20). Additionally, the slow diffusion of the

medicine as well as the fast turnover rate of the cerebrospinal fluid (CSF) can lead to a quick clearance of the substance in the CNS, delaying or even ceasing the therapeutic effect (22).

For these reasons, to achieve long-lasting therapeutic results on the brain, the blood-brain barrier must be circumvented, and non-invasive strategies need to be devised to provide therapeutics agents to the brain efficiently. In consequence, one of the best ways to bypass the BBB and contribute to a more efficient drug delivery is the nose-to-brain pathway. Such route allows for an increase in the patient compliance and an easy administration without the need of trained professionals nor a hospital setting. A rapid onset of action and minimal systemic exposure also occurs, conceding a decreased risk of adverse effects (23). In addition, the usage of the nasal mucosa to deliver medicine into the brain permits an escape to the gastrointestinal tract's acidic environment and enzymes as well as the enabling of an avoidance of the first-pass effect, being the nasal doses about 2-4 times lower than the oral doses (21,23).

1.3.1 Blood Brain Barrier

The treatment of multiple neurological diseases has been difficult as 98% of the current marketed medicines are ineffective in treating them (20,24). As the CNS is one of the most important and complex systems in the organism, it is important an assembly of competent and sturdy group of cells that enable an efficient safeguarding of it. The existence of the blood brain barrier leads to this occurrence. This restricting structure is composed of different types of cells that come together to regulate the homeostasis of the central nervous system (CNS) as well as to shield the brain from toxins and pathogens, avoiding a possible infection/disease (25).

Putting some emphasis on the brain capillaries, these are made of a monolayer of endothelial cells although they tend to be substantially different than the peripheral capillaries of another non-neural tissues: they lack the presence of fenestrae and are continuous, exhibiting the highest level of restriction concerning the movement of solutes (25).

Besides this characteristic, these cells contain a luminal and an abluminal membrane, each containing different types of mediated transporters. Such categorization qualifies

them to be polarized, another condition enabling a more selective environment regarding the substances that can pass through the BBB. It is known that the abluminal membrane contains the ATP-dependent sodium pump that is fundamental for the homeostasis of the CNS whereas the luminal side contain P-gp systems. These proteins must be considerate as they are one of the most efficient setups to protect the CNS from harmful molecules (18). However, it is equally important to consider the paracellular pathway. This route is led by tight junctions, located on the EBC, structures that allow the passing of molecules intercellularly in a passive way against the concentration gradient and are very selective on which substance to pass on, being the only molecules able to do so lipophilic molecules under 400-600 Da and some solutes such as oxygen and carbon dioxide (24). These structures play a crucial rule on differentiating peripheral capillaries from neural ones.

Following the microvasculature, there is matrix called basal membrane that is responsible for either creating an additional protective shield of the molecules when moving across the blood towards the neural space and involved in several signaling processes.

Brain endothelial cells are capable of various types of transport: the paracellular pathway, that is the passing of solutes, ions and certain molecules led by the tight junctions of the endothelial cells themselves as well as the transcytosis/pinocytosis that are held by several substrate-specialized mediated transcellular transports such as receptor-mediated transcytosis, cell-mediated transcytosis, transporter-mediated transcytosis, and adsorptive mediated transcytosis. Figure 3 illustrates the several types of transport mentioned (20).

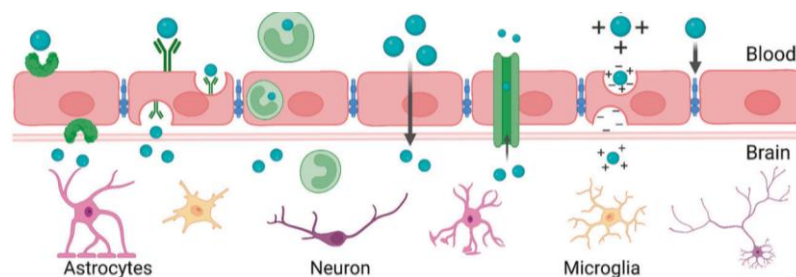


Figure 3: Schematic diagram for different mechanisms for BBB crossing. Adapted from (20).

Additionally, macrophages, neutrophils and T-cells can also interact with the brain blood vessels and release reactive oxygen species. These circumstance causes inflammation towards the BBB and can be the origin of several neurological diseases (25). Figure 4 represents an illustration of the BBB layers.

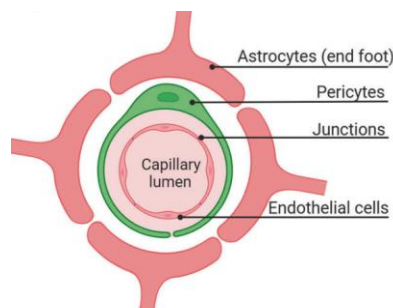


Figure 4: Schematic diagram of BBB structure. Adapted from (20).

1.3.3 Nasal Anatomy

Before delving into the concept of the intranasal route itself, it is important to recap some basic concepts of the nasal anatomy. Therefore, the nasal system is composed by three main regions: the nasal vestibule, the entrance of the nose, the respiratory region and the olfactory region (26). The respiratory region and the olfactory region will be taken more into account as they possess the main structures for such route.

The area with the most surface area is the respiratory region. Its main function is to warm the inhaled air as well as filtering allergens and microorganisms. Also, the fact this region is highly vascularized makes it also interesting to consider when it comes to systemic drug delivery (27). It is on this region where the mucociliary clearance takes place as this locale is composed of ciliated, non-ciliated, basal and Goblet cells (22). This concept is important when developing intranasal formulations as they should penetrate the nasal mucus and adhere to the local epithelium to minimize mucociliary clearance. Also, once the drug passes the mucus, the subsequent permeability of the nasal epithelium should optimistically improve. Another fundamental important factor to consider amongst this area, if not the most important, is the trigeminal nerve. It starts on the respiratory epithelium and ends in the brain, being responsible for an intracellular pathway for nose-to-brain drug delivery (22,27).

Lastly, the olfactory epithelium is located in the upper part of the nasal cavity approximately 7 cm from the nostrils and its composition varies between olfactory

sensory neurons and sustentacular or supporting cells that are responsible for the ensheathing of the receptor. It is important to assert these cells are interspaced between each other, granting the intracellular and the extracellular pathway that will later be discussed. Plus, this region has olfactory nerves which allows a direct connection to the brain enabling the drug to reach several parts of the brain bypassing the BBB, incorporating the intracellular pathway and the extracellular pathway (26,28).

1.3.3.1 Intracellular pathway

The most relevant pathway for a drug to reach the CNS via intranasal is through neuronal connections. (27). Accordingly, there are two routes involved in the delivery of drugs into the brain involving the nerves: the intracellular route, having the olfactory and the trigeminal nerve as a resource whereas the extracellular one is predominantly enabled by the olfactory nerve.

If the drug goes through the olfactory nerve, it can either undergo a process of endocytosis through such structure and terminate in the olfactory bulb, representing the intracellular route, taking about 1.5-6h to reach the brain (20).

Regarding the trigeminal nerve, when intranasally it will cause the endocytosis of the drug via the ophthalmic and the maxillary branch, reaching the bulb stem directly. It can also exhibit an extracellular route by bulk flow processes, but such is not the most prominent pathway (27).

1.3.3.2 Extracellular pathway

The extracellular route comprehends a paracellular transport between the olfactory neurons and the supporting cells with the drug being distributed directly into the CSF of the subarachnoid space and consequently the brain. However, the fact tight junctions of such cells must be overpassed can limit the uptake (27,28).

Along the olfactory axon bundles, arteries provide nutrients to supply the nerves. Such arteries contain a perivascular pump by systolic-associated high pressure that can increase the velocity of the drug transport and reduce reaching CNS time through the olfactory nerve from 6h to 0.33h and from 56h to 1.7h when taking the trigeminal nerve course, making these feasible routes to deliver medicines (27).

Figure 5 represents an illustrated scheme of the olfactory and the respiratory routes.

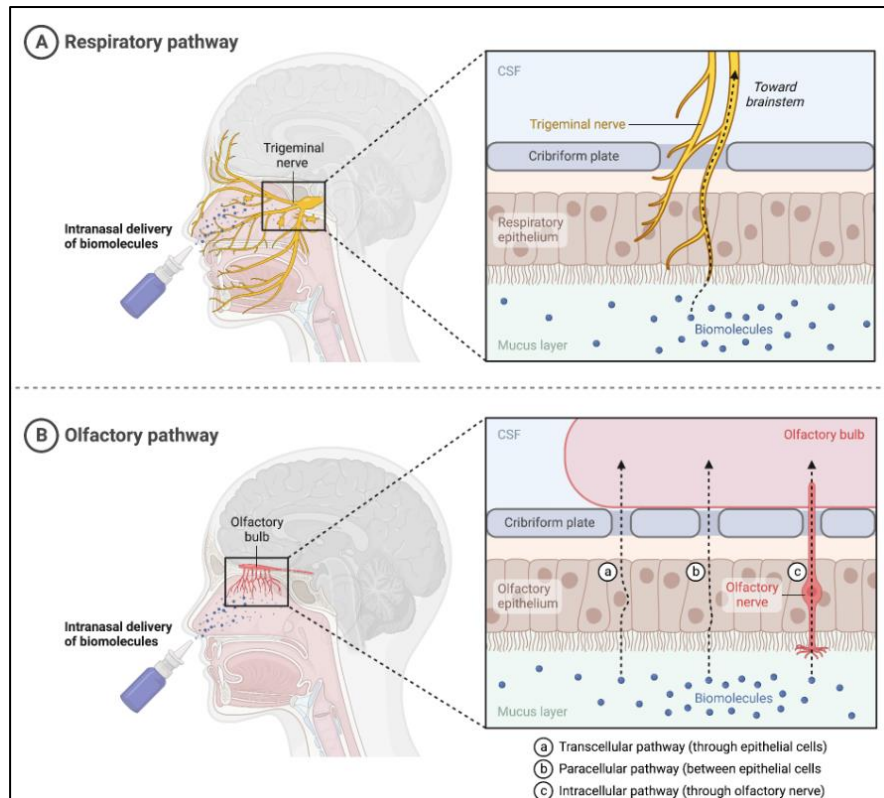


Figure 5: Direct nose-to-brain routes. Adapted from (29). **A)** Respiratory pathway: the intracellular medicine transport can occur in this region by the trigeminal nerve located both in the respiratory as well as in the olfactory region. **B)** The olfactory pathway comprises the intracellular pathway (transcellular and through the olfactory nerves) and the extracellular/paracellular pathway between epithelial cells.

1.3.4 Nanoparticles in Nose-to-brain delivery

The delivery of nanotechnological medicine to the brain via the nasal cavity pathway was proposed not only because of the advantages such route portrays but also because other paths might not be the most convenient. It is believed that the reticuloendothelial system, composed by several mononuclear cells with a phagocytic function, has the ability to remove about 85% of nanoparticles from the vascular space when given intravenously. Thus, such action enables a reduced NP exposure to the cerebrovascular and a decreased concentration of the pharmaceutical in the brain (30).

Due to the unique anatomical relationship between the CNS and the nasal cavity, the intranasal route is a quick and an easy access for certain medicine to be delivered into the brain (20).

Regarding DMF, this pharmaceutical has been showing efficacy in treating MS, however, the pharmaceutical is taken as an oral form, and it has been reported to be unstable in gastrointestinal milieu as well as causing a gastrointestinal irritation. Another important issue to consider is that the multiple dosing, taken 2 times a day, presents a poor adherence of the patient to the treatment and a compromised brain permeability (1).

Rutin is also a lipophilic medicine however the solubility is low which makes the oral form not convenient to the delivery (31).

The intranasal delivery is aimed at optimizing drug bioavailability for systemic drugs, as absorption decreases with increasing molecular weight, and for medicine that is susceptible to enzymatic degradation such as proteins and polypeptides.

Nanoparticles may offer an improvement to nose-to-brain drug delivery as the encapsulated drug is protected from biological and/or chemical degradation, as well as by P-gp efflux proteins present in the BBB. Besides this fact, a high relative surface area means that these nanocarriers will release drug faster than larger equivalents (22).

It is known that the olfactory axonal diameter of humans is in the range of 100-700 nm and nanoparticles, when larger than about 20 nm, are thought to pass transcellularly in nose-to-brain drug delivery pathway (22,32).

In intranasal administration to the brain, a particle size between 10 and 300 nm is advantageous since nanoparticles this size can be transported directly by the olfactory nerve to the brain (33).

Previously, Pardeshi *et al* innovated and performed a lipid-polymer hybrid nanoparticle containing ropinirole, an Alzheimer's disease hydrophilic medicine. Their study was conducted to identify whether it is feasible to either carry such molecule in the nanoparticle category as well as via intranasal. The nanoparticles were processed using a modified emulsification-solvent diffusion technique and physicochemical results showed the optimal formulation presented minimum particle size with this parameter ranging from 98 nm to 287 nm with a polydispersity index (PI) within 0.011 and 0.38 (34).

With this, the results are agreeing with literature studies regarding the optimal size of NP to have an intranasal delivery; The fate of nanoparticles in the endocytic pathway is dependent on the size and surface characteristics of the particles (22).

1.4 Colloidal drug delivery systems

As technology and medicine tend to evolve throughout the years, many innovative systems have been developed to help deliver drugs in a non-invasive, efficient and secure way. Such evolution is required due to the low biodistribution as the therapeutic potential is not fully achieved and the amount of side effects to healthy donors is significant (35).

Throughout the last 30 years, colloidal drug delivery systems (CDDS) have been created and progressed to bypass the issues mentioned above as well as improving the drug targeting, execute a controlled drug release and prevent either hydrolysis or enzymatic degradation (36).

Within this group there are nanomedicines, or medicines using nanocarriers (NC), that are intended to function as vectors of several active substances and control their biodistribution. Beyond this parameter, these carriers present several advantages such as an increased deposition of drugs at the target site and a higher concentration of the medicine intracellularly; a sustained and controlled drug release can be achieved which can lead to the reduction of side effects and potential toxicity (35,36).

1.4.1 Nanoparticles

Composed by sub nanosized colloidal structured, nanoparticles (NP) are defined as particles with one dimension ranging between 1 and 1000 nm having different properties depending on their surface functionalities (30,37).

NP are gaining relevance as key roles for either clinical application or diagnosis (37).

The inherent potential of nanoparticles for therapeutic cargo delivery is primarily attributable to a few key parameters, including average nanometric size, homogeneity, surface potential, and drug loading, among others. (38)

Based on chemical and physical characteristics, they can be categorized into several groups including liposomes, solid-particle NP and polymeric-nanoparticles (39).

1.4.1.1 Polymeric Nanoparticles

This kind of particle is created through the self-assembly of a polymer with both hydrophobic and hydrophilic regions. The hydrophilic region can form the shell of the particle, while the hydrophobic region constitutes the core. As a result, hydrophobic and poorly soluble drugs can be incorporated into the hydrophobic core, effectively increasing their solubility and circulation time (40).

One of the most common polymer used is poly lactic glycolic acid (PLGA), however natural polymers are widely used as Govender *et al* were able to incorporate tetracycline into a chitosan nanoparticle for periodontal therapy, increasing the NP stability (37,41). Another study conducted took place in 2016 when Ahmad *et al* produced mucoadhesive polymeric nanoparticles with the goal of enhancing the nasal residence and the slow release of drug supply to brain at a constant rate (16).

1.4.1.2 Liposomes

Another category of the nanoparticles' spectrum is the lipid-NP, or liposome. Liposomes are self-enclosed spherical structures, composed by a phospholipids and cholesterol bilayer with an aqueous core. Their size range initiates at 20 nm and its arrangements allows an extended circulation time as well as a good storage stability (36,42).

Another advantage of this NP is the practical manufacturing methods as well as a low-cost process.

An association between the lipid component with a polymer, specifically polyethylene glycol (PEG) enabled an increase in the half-live of the NP and its stability (37,39).

Doxil and Myocet are two liposome-based medicine containing doxorubicin, an anti-cancerous agent, approved by the FDA (39).

1.4.1.3 Lipid-Polymer Hybrid nanoparticles (LPHNP)

Regarding the lipidic NPs, even though owning a plethora of advantages, there are some factors that condition their application, like i) drug-loading capacities; ii) Low membrane retention properties, iii) the physical state instability of lipids and iv) the loss of the fluidity of cell membranes also contributes for the stability-poor properties

of this type of NP, phenomenon that occurs especially during storage and administration (43).

The consequence of such processes is the mislaying of the drug and neutralization of the potential therapeutic effects.

Polymeric NP, apart from also portraying a series of interesting properties to drug delivery as mentioned above, can also display toxic monomer accumulation and degradation and drug leakage before reaching the target (Lockman et al., 2002). Besides, the difficulty in upscaling such NP to the adaptation of production technologies also another concern (44).

On behalf of these factors, a new category was created to achieve a controlled drug delivery and enhance the stability of the particle (45).

Consequently, the Lipid-Polymer hybrid nanoparticle was developed (38).

This group of nanoparticles reflects a union between a polymeric-NP and a liposome, being the main goal to benefit of the special properties of polymeric nanoparticles and liposomes that contributed to their early therapeutic effectiveness. At the same time, limitations of these systems are also being addressed such as the disintegration that may occur and the material leakage (38,40).

Drug releasing of the drug is regulated by the polymer whereas the lipidic material enhances the permeation of the particle across the membrane (39).

In literature there are many articles expressing the benefits of LPHNP. Specifically, Kaczmarek *et al* were able to improve the stability and efficacy of mRNA-containing particles to mice lungs with the resource of LPHNP. In order to maintain new hydrophobic interactions, to Poly(β -amino esters) (PBAEs), a polymer, alkyl amines were added, allowing for a formulation with a polyethylene glycol-modified lipid (PEG-lipoid). Results showed an increase of the stability of the nanocarrier at physiological conditions. (46)

Another advantage of these nanoparticles is the appropriate cellular and molecular targeting (38,39).

1.4.1.4 Composition of LPHNP

Lipidic-polymeric hybrid nanoparticles can be classified into two types based on their hybrid nanoscopic structure and assembly methods: Type-I monolithic matrix and Type-II core-shell systems (47).

Even though there are different assemblies in which such nanoparticles can be arranged, the novel generational delivery drug system and architecture in which this experiment was conducted is not the usual polymeric core and lipidic shell arrangement widely reported (38,42).

Thus, the general formulation of the nanoparticles under experiment consists of a lipidic core and a polymeric-shell (LCPS). In these systems, the core includes a lipidic component enclosed by one or multiple polymeric coats. The kernel holds the API (active pharmaceutical ingredient), and the shell stabilizes the core by overcoming biological obstacles (48).

The projected formulations are designed by having *phosphatidylcholine* ≥ 94.0 % (PC) as a lipid-kernel and a hyaluronic acid (HA) polymeric-based shell. Regarding the API, dimethylfumarate and rutin are encapsulated within the lipidic kernel as they both present a hydrophobic nature. To enhance solubility and bioavailability concerns, DMF and rutin will be incorporated into LPHNP (Lipid-Polymeric Hybrid Nanoparticle) as a nanocarrier. The goal is to maintain solubility in the blood while facilitating the delivery into the CNS. Figure 6 comprehends an illustration of the projected structure of LPHNP formulated in this study.

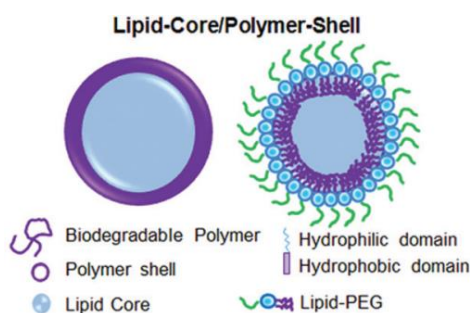


Figure 6: Lipidic-core polymeric-shell nanoparticle. Adapted from (47).

1.4.2 Methods for LPHNPs preparation

On the purpose of obtaining hybrid nanoparticles, numerous processes have been described in the past years. Accordingly, LPHNP can be obtained via the single-step

method, consists of mixing polymeric and lipidic solutions that self-assemble to form LHNPS. Some of the techniques are nanoprecipitation and emulsion-solvent-evaporation (49). However, novel techniques were studied in the monography: modified nanoprecipitation and modified nanoprecipitation with the resource of a syringe pump.

1.4.2.1 Modified Nanoprecipitation: Sonication

Nanoprecipitation, also known as solvent-displacement method, is an innovative, rapid and easy to perform technique to obtain nanoparticles in an instantaneous and only step way (50).

This referenced method, developed by Fessi (51) includes the dispersion of lipids in aqueous phase via sonication or heating (52). Sonication will take place for the nanoparticles' synthesis.

Briefly, this methodology requires two miscible solvents with the drug and the polymer dissolved in the first one but not in the second (non-solvent). Consequently, the polymer-solvent desolvates when added into the non-solvent and diffuses into the dispersing medium, precipitating and entrapping the API (50).

However, in this study, the polymer was dissolved in water (solvent) and the API was entrapped within the organic phase with ethanol as a non-solvent.

An oil-in-water dispersion was executed with the hydrophilic polymer, HA, dissolved in water rather than an organic miscible with water solvent. In terms of the organic phase, the lipophilic excipients have been dissolved in ethanol as the solubility with water is bigger than 2%, making it a feasible solvent to enable the precipitation of the polymer and its consequent evaporation.

The fast nanoparticle formation is ruled by Marangoni effect, which is subjected to interfacial turbulences that occur at the interface of the solvent and the non-solvent and results from complicated and cumulated phenomena like flow, diffusion, and surface tension variations (53). Thus, this technique is easy, less complex and requires less consumed energy and another advantage is the fact this approach is not limited to a specific polymer but can be extended to synthetic or natural polymers (54).

The difference between this method and others written in literature is the fact that we did not utilize both immiscible in water solvents, but one solvent is water and the

other one an organic solvent, ethanol. Additionally, the polymer and the API were not dissolved together in the water but were dissolved previously in the organic phase.

1.4.2.2 Modified Nanoprecipitation: Syringe Pump Method

In this experiment, hyaluronic-acid LPHNP were created with the solubilization of either the polymeric solution and lipidic solution, having Poloxamer F407 as a surfactant to stabilize the dispersion.

With the realm of literature, besides lipidic and polymeric components, a multitude of factors have been known to influence the nanoparticles size. These parameters spans from the solvents choice to process variables, like the injection speed of ethanol, the flow rate of the water as well as hydrodynamic forces and their distribution with respect to interfacial position which influences the particle formation. These concerns are significantly dependent on the operator, posing challenges to control them (54).

For these reasons, the employment of an automated system for nanoparticle synthesis can avoid this dependency by optimizing the process while at the same time enabling the scale-up of this technique (54).

The syringe pump method is an innovative technique that allows a dropwise of the organic phase into the water solvent without high-energy/high-shear/high-pressure properties enclosed. The details of the programmed device is detailed at the 3.1.2 Section.

1.4.2.3 Excipients of formulations

The choice of the excipients of the formulations should be considered as it must not be any incompatibility between either the excipients or the API. Therefore, as nanoparticles will be produced and as previously explained, they will be divided by an organic phase and a water phase.

Regarding the organic phase, and as already displayed, the main components will be: *phosphatidylcholine* ≥ 94.0 % (PC), derived from soybean. Its main function is to act as a stabilizer on the oil-in-water dispersion.

To compose the main component of the lipid kernel, to some samples PC will be replaced by a PEGylated-lipid, more specifically the lipid-PEG 2000. The advantage of the PEGylation of the lipid is the enablement a longer circulation half-life because the NP escape capture and phagocytosis by various organs (48).

Cholesterol is another excipient utilized in the experiment for the organic phase. As a natural phospholipid and present in the bilayer of membrane cells of the human species, such molecule, if used in a formulation, has been reported to prevent aggregation in the aqueous environment as well as to improve the stability of the formulation. Such phenomenon occurs as cholesterol can prevent the phase transition of phospholipids within the nanoparticle (55,56).

The main stabilizer considered to belong to these formulations is the Poloxamer 407, an amphiphilic non-ionic surfactant that presents low toxicity, irritation and immunogenicity (57,58). As the temperature rises, Poloxamer molecules aggregate into micelles and have an emulsifier and stabilizer function in the referred drug delivery system (58).

Defined as a copolymer, the structure of the component is arranged as a triblock structure of polyethylene oxide (PEO) and propylene oxide (PO) blocks arranged in a triblock structure $PEO_x-PO_y-PEO_x$, with x being 95-45 and y 54-60. These values are important as they confer an HLB (hydrophilic-lipophilic balance) of 22 conferring the molecule a hydrophilicity. Due to the hydrophobic PO core, this molecule promotes the solubilization of poorly-water soluble drugs, like DMF and rutin (59). Thus, this adsorption mode enables for the hydrophilic PEO side-arms to stay in a mobile state as they extend outward from the particle surface. This concept provides stability to the nanoparticle by a repulsion effect through a steric mechanism of stabilization involving both enthalpic and entropic contributions (60).

Palmitoylethanolamide 95% (PEA) is an endogenous endocannabinoid-like bioactive lipid mediator located in several tissues including the brain (61). Its function reaches several fields as it can maintain an anti-inflammatory and neuroprotective action in several pathologies including neurodegeneration, being able to cross the BBB (62). However, in this study, PEA was used as an excipient to stabilize the lipophilic bilayer of the nanoparticles because of the similar properties.

1.5 Hyaluronic acid

1.5.1. Composition

Hyaluronic acid (HA), also known as hyaluronan, is a linear anionic polysaccharide composed of repeating units of disaccharides d-glucuronic acid (GlcA) and N-acetyl-

d-glucosamine (GlcNAc) linked together through alternating β -1,3 and β -1,4 glycosidic bonds (63). Figure 7 illustrates hyaluronic acid's molecular structure.

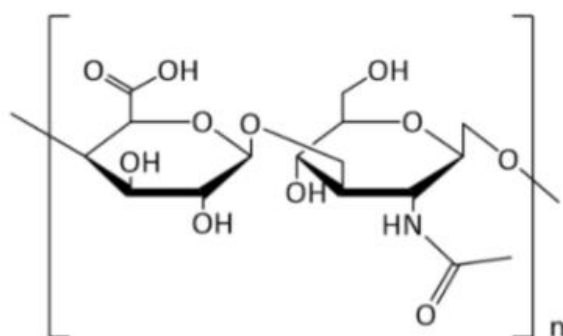


Figure 7: Molecular structure of Hyaluronic Acid. Adapted from (64).

Main component of the extracellular matrix (ECM), it is also present in the skin, the vitreous humor and synovial fluid of vertebrates (63,64). Although it has a natural production, microbial fermentation has been used with the aim of producing HA (63).

One of the the synthesis process of HA is obtained by three HA synthases (HAS). HAS-2 can predominantly create High Molecular Weight hyaluronic acid (HMW-HA). This molecule has a size range from 200-200 kDa. Presenting anti-inflammatory and anti-cancerous activities, Tian *et al* demonstrated such concept by knocking down HAS-2 in naked mole rat cells and observing the susceptibility of malignant transformations increasing (65).

1.5.2 Hyaluronic Acid as medicine carrier

HA is a natural molecule produced by the organism itself; thus, its biodegradability, biocompatibility, lack of toxicity and non-immunogenic properties make it enthusiastic for biomedical applications and diseases in cancer, lung injury, diabetes (64).

Previously, on the matter of breast cancer, Suksiriworapong *et al* were able to develop hyaluronic-acid surface-coated lipidic-polymeric hybrid nanoparticles of *Cordyceps militaris* herbal extract to treat such pathology. The architecture of the NP was a polymeric-core lipidic-shell using poly(glycerol adipate) (PGA) as a polymer and phosphatidylcholine as a lipid. The results showed an enhanced anti-cancer activity against oncogenic cells, meaning the conjugation of HA in LPHNP is a reliable approach to consider (66).

As the olfactory pathway is the most prominent route of intranasal transport, there must be an optimal adherence to this nasal region to ensure an optimal drug penetration. The mucociliary clearance occurs every 15-20 minutes, so mucoadhesive NP must be developed to facilitate the absorption through the mucosal membrane by expanding the residence time in the nasal cavity and proceed with the olfactory transport (67).

Throughout literature, research on mucoadhesive core-shell nanoparticles, composed by organic or inorganic cores surrounded by HA corona, have been proposed to deliver drugs or gene materials, with the goal of restricting the mucociliary clearance and maximize the therapeutic potential of the gene/API (68).

Regarding neurodegenerative diseases, studies have been done with this polysaccharide. In the realm of Alzheimer's disease, nanoparticles have been designed for nose-to-brain delivery to hinder the systemic effects. The goal was to transport RNA molecules in an octaarginine and lactic acid conjugation, enveloped by a hyaluronic acid shell. This coat was intended to improve the nanoparticles' stability and mucodiffusion across the olfactory nasal mucosa. The results were promising as an unimodal size distribution with an adjustable mean size was achieved and the RNA was protected from degradation (69).

2 Aim of Study

This study was conducted to analyze the physicochemical properties of lipid-polymer hybrid nanoparticles utilizing phosphatidylcholine as a lipid-core material, hyaluronic acid as a polymeric-shell, PEA and cholesterol as stabilizing agents as well as Poloxamer F407 to avoid aggregation formation. Such nanoparticles will be carrying individually two different drugs to be intranasally administered, more specifically: dimethyl fumarate and rutin, entrapped in the lipidic kernel.

Additionally, two different methods were utilized to develop the nanoparticles. The first method consists of a modified nanoprecipitation with the resource of the sonicator.

The other process consists of the execution of a modified nanoprecipitation with the resource of an infusion single syringe pump. Both processes were followed by an organic solvent evaporation (ethanol) at room temperature.

Thus, the reliability of such processes will be analyzed to determine which one is more feasible.

14 formulations (LCPS-1 to LCPS-15) were developed with different quantities of lipidic and polymeric excipient, with and without API. The main objective was to evaluate the different percentages of each excipient that could effectively carry the active pharmaceutical ingredients within the NP in the most efficient way, being nanoparticle size, polydispersity Index and drug loading the assessment parameters.

Potential zeta is also an important parameter to assess however it was not evaluated due to the unavailability of the equipment needed.

To determinate the drug loading efficiency of DMF and rutin, the content was analyzed via High Performance Liquid Chromatography (HPLC) and UV spectrometry, respectively.

3 Materials and Methods

3.1 Materials

3.1.1 General Materials

- Beakers (5 mL, 10 mL)
- Glass pipette
- Pasteur pipette
- Analytical balance ABJ 220-4M, Kern and Sohn GmbH, Germany
- Heating plate
- Magnettos
- Digital Thermoregulator Vortex, TechnoKartell, Milan, Italy
- Filtration Equipment with Nylon Filter 0,45 uM
- Submicron Particle Size Analyzer, Beckman Coulter N5, Beckman Coulter, USA.
- Photodiode Array Detector, Varian Prostar 330, Varian, USA.
- Autosampler Varian ProStar 410 HPLC, Varian, USA.
- Solvent Delivery Module, Varian ProStar 210, Varian, USA.
- Precision CELLS made of Quartz SUPRASIL, Hellma GmbH & Co. KG, Germany.
- Exacta Optech Spectrophotometer cells, Exacta Optech GmbH, Germany.
- Shimadzu UV-1800 UV/Visible Scanning Spectrophotometer, Shimadzu, Japan.

3.1.2 KD Scientific Single Syringe Infusion Pump

For the nanoprecipitation of the nanoparticles, the syringe-pump instrument (KDS 100 Legacy single syringe infusion pump, Massachusetts, USA) was used.

This equipment consists of a durable construction welded seams, a prevent syringe damage–guide rod clamp, a backlit LCD, simple syringe installation, and a quick release drive nut.

The power switch is located at the right, rear corner of the pump.

Regarding the syringe volume, it is about 10 μ l to 60 ml, being filled with 5 mL for this study.

For the setup and pump operation, a menu is displayed on an alphanumeric LCD enabling the operator to make the necessary selections using the keypad for choice of features and numerical entries.

The internal diameter of the syringe is used by the control program to calibrate the pump and deliver the volume and flowrate selected. Another aspect to consider is the syringe diameter, which is also used to set automatically the volume and flowrate units.

The syringe diameter can be entered directly, or the syringe can be identified from a table of syringes held in memory. When the syringe is selected from the table the diameter is entered automatically. There are two dispense modes:

Dispense volume mode, in which the pump keeps track of the volume dispensed and automatically stops the pump when a set target volume is reached.

Run mode, where the pump runs at the set flowrate until manually stopped, which was the chosen mode for the experiment. In the event of a power interruption during operation, the pump can be programmed to either resume operation or remain stopped when power is returned. The pump settings were stored in memory to minimize the number of setting changes required, allowing for a more accurate process.

To facilitate loading, the pusher block [1] can be released from the leadscrew and manually moved along the guide rods to accommodate the syringe. Press the bronze release button [2] on the side of the black pusher block [2] to release the block from the leadscrew. Raise the spring-loaded retaining clamp knob [3] and rotate away from the syringe barrel. Place the syringe barrel in the V of the syringe holder, making sure that the flange of the syringe barrel is pressed against the side of the syringe holder. Rotate and release the syringe clamp to hold the syringe in place. Press in release button [2] and move the pusher block back along the guide rods to contact the syringe plunger (70).

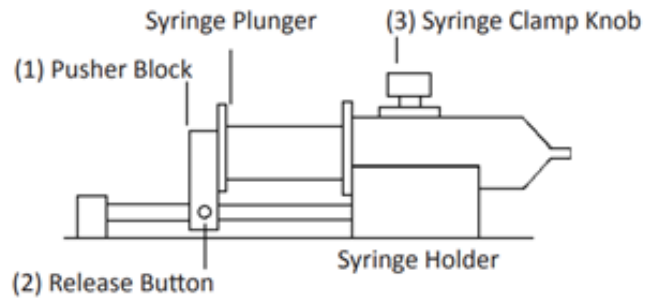


Figure 8: Schematic picture of the KDS 100 Model Scientific Single Syringe Infusion Pump. Adapted from (70).

3.1.3 Chemicals

Table 1: Components of the water and organic phase.

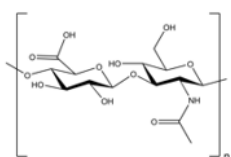
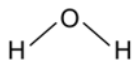
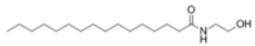
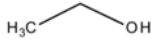
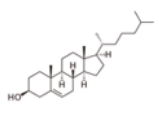
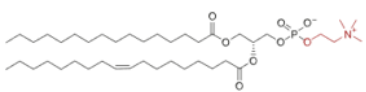
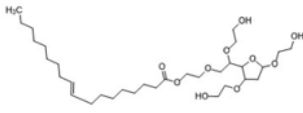
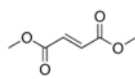
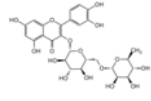
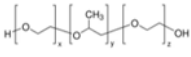
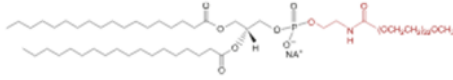
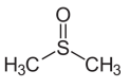
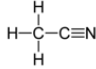
	Chemical	Chemical formula	Molecular structure
Water phase components	Hyaluronic Acid	$(C_{14}H_{21}NO_{11})_n$	
	Water	H_2O	
	Palmitoylethanolamide	$C_{18}H_{37}NO_2$	
Organic phase components	Ethanol	C_2H_6O	
	Cholesterol	$C_{27}H_{46}O$	
	Phosphatidylcholine	$C_{18}H_{37}NO_2$	
	Tween 80	$C_{64}H_{124}O_{26}$	
	Dimethyl Fumarate	$C_6H_8O_4$	
	Rutin	$C_{27}H_{30}O_{16}$	
	Poloxamer F407	$(C_3H_6O.C_2H_4O)_x$	
Lipoid-PEG 2000	$C_{133}H_{267}N_2O_{55}P$		

Table 2: Chemicals used for the loading analysis of the API.

Chemical	Chemical formula	Molecular structure
DMSO	C_2H_6OS	
Acetonitrile	C_2H_3N	

PEA 95%, Cholesterol and Poloxamer F407 were purchased from Sigma-Aldric from Merck (USA). Water was obtained from Mili-Q water Purification System, MilliporeSigma. PC and Lipoid-PEG 2000 was gifted by Lipoid GmbH (Ludwigshafen, Germany). Hyaluronic acid sodium salt from BioChemical Fluka. Acetonitrile, DMSO and Ethanol and were obtained by Sigma-Aldrich (Milan, Italy). All other chemicals used were of analytical grade.

3.2 Methods

3.2.1 Preparation of LPHNP

3.2.1.1 Water phase preparation

Generally, hyaluronic acid was weighted (Kern Analytical balance ABJ 220-4M) and dissolved in distilled water to serve as the diffusing phase. As HA only dissolves at lower temperatures, ice was used to dissolve such molecule and put in the plate for 30 min at 4°C while ongoing continuous magnetic stirring.

2 mL of Poloxamer 0,5% (w/w) and 3 mL of water were then added to the solubilized water phase. Such step enables the Poloxamer to rigidify the polymeric component of the nanoparticle by interacting with the HA.

However, LCPS-8, LCPS-11 and LCPS-14 do not have hyaluronic acid incorporated, only 3 mL of Poloxamer 0,5% (w/w) and 7 mL of water were added to water and solubilized.

3.2.1.2 Organic phase preparation

In this phase, the excipients were weighted (Kern Analytical balance ABJ 220-4M) and dissolved in ethanol at 50°C followed by continuous stirring with a magneto and an agitation plate.

LCPS-2 had every organic phase component weighted and solubilized in ethanol with the same parameters however after solubilization was done the surfactant Tween 80 was added to the previously solubilized oil phase whereas Poloxamer F407 was the surfactant applied in LCPS-1 and the remaining formulations. Afterwards, the dispersion took place with the resource of the vortex (Digital Thermoregulator Vortex, TechnoKartell, Milan) at 35 Hz in 2 min.

The Water:Ethanol ratio of LCPS-1 to LCPS-4 is 1:1. However, in LCPS-5 to LCPS-15 this ratio increases to 2:1.

After solubilization of the organic phase components, to formulations LCPS-7, LCPS-8 and LCPS-15 DMF was loaded and rutin was loaded in formulations LCPS-13 and LCPS-14.

The quantities of the excipients on every formulation are written in table 3.

Table 3: Percentages of components and methodology of LCPS-1 to LCPS-15.

Formulation name	Organic phase EtOH							Total amount of the phase	Water phase Water		Methodology
	PEA	PC	Lipoid-PEG 2000	Cholesterol	Poloxamer F407	DMF	Rutin		HA	Polox 0,5% (w/w)	
LCPS-1	+	-	+	+	+	-	-	12 %	+	-	Modified Nanoprecipitation: Sonication
LCPS-2	+	-	+	+	Tween 80	-	-	12%	+	-	
LCPS-3	+	-	+	+	+	-	-	13 %	+	-	Modified Nanoprecipitation: Syringe Pump Technique
LCPS-4	+	-	+	+	+	-	-	10%	+	-	
LCPS-5	+	-	+	+	+	-	-	10%	+	+	
LCPS-6	+	+	-	+	+	-	-	10%	+	+	
LCPS-7	+	+	-	+	+	+	-	11,8%	+	+	
LCPS-8	+	-	+	+	+	+	-	12,8%	-	+	
LCPS-9	+	-	+	+	-	-	-	10%	+	-	
LCPS-10	+	+	-	+	+	-	-	12%	+	+	
LCPS-11	+	+	-	+	+	-	-	12%	-	+	
LCPS-12*											
LCPS-13	+	+	-	+	+	-	+	12,4%	+	+	
LCPS-14	+	+	-	+	+	-	+	12,4%	-	+	
LCPS-15	+	+	-	+	+	+	-	12,8%	+	+	

*: LCPS-12 was not feasible for analysis.

3.2.1.3 Modified Nanoprecipitation: Sonication

Regarding LCPS-1 and LCPS-2, such formulations were executed with the resource of a vortex (Digital Thermoregulator Vortex, TechnoKartell). In this experiment, both phases when dissolved were subjected to an ultrasonic technique through a sonication process: the period of time was 2 min with 50 Hz after a minute stop period and then another 2 min.

3.2.1.4 Modified Nanoprecipitation: Syringe Pump method

The methodology to create nanoparticles from LCPS-3 to LCPS-15 was the modified nanoprecipitation with the resource of the syringe pump.

In this process, an Infusion Syringe Pump (KDS 100 Legacy single syringe infusion pump, Massachusetts, USA) was utilized. For this, 5 mL of the oil phase filled the syringe being then forced through the needle (inner diameter: 11.99 mm) at 333.3 $\mu\text{L}/\text{min}$ and a flow rate of 3.3 mHz. A nanoprecipitation began with the dropwise of the organic phase into the water phase that was continuously stirring in the agitation plate with the help of continuous stirring agitation at room temperature.

3.2.1.5 Solvent evaporation

After both processes were finished, the final preparations were then air-dried with the help of the magneto and the agitation plate for 5 hours at room temperature. This process is important for the evaporation of the organic solvent, ethanol. Such solvent presents a higher than 2% solubility with water, making it an ideal solvent for the rapid precipitation of the nanoparticles as well as an ideal solvent evaporation of the remain of it. Besides, this choice prevents the use of halogenated organic solvents, like dichloromethane as they have a higher toxicity.

Figure 9 represents a diagram of the proposed methodology to obtain the nanoparticles.

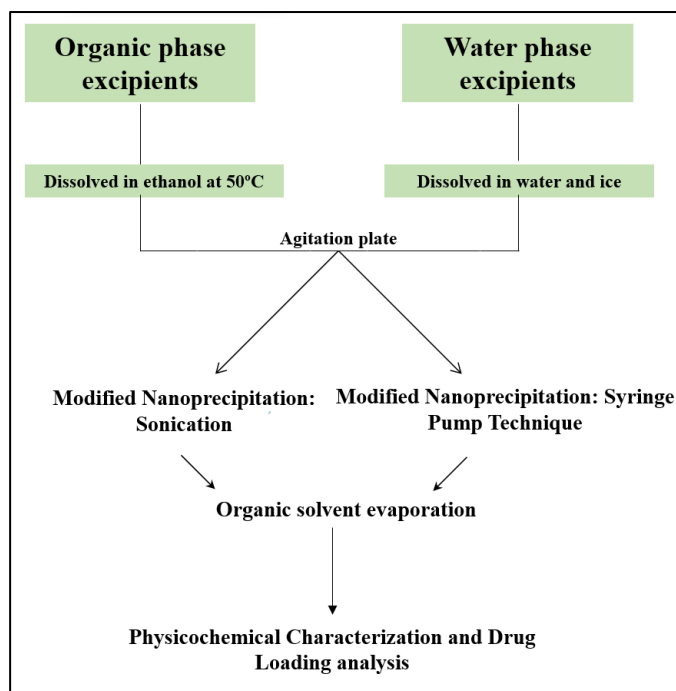


Figure 9: Diagram of nanoparticle's scheme.

3.2.2 Physicochemical characterization of the nanoparticles

3.2.2.1 Particle Size

With the aim of characterizing the nanoparticles in the particle size matter, the methodology applied was the laser light scattering photon correlation spectroscopy and the instrument utilized was the Beckman Coulter N5 Submicron Particle Size Analyzer.

10 μL of the samples were first filtered with a 0,45- μM filter and injected into a quartz cell directly into the instrument. Each sample was analyzed in triplicate to ensure reproducibility and the process occurred at room temperature. Between each measurement the cuvettes were washed out with distilled water.

3.2.2.2 Polydispersity Index

To assemble the dispersity of the particle sizes, the method and instrument employed were the same as the particle sizes' and each sample was analyzed in triplicate to ensure reproducibility.

3.2.2.3 Stability over time

The samples were refrigerated in a fridge between 2 and 8°C for four months. At certain times, the formulations were drawn and the particle size and PI were assessed and analyzed.

3.2.3 Drug loading of the API

The percent drug loading is essential because it influences the release characteristics of the drug molecule.

Drug loading efficiency is the mass of drug entrapped within the particles relative to the total mass of NP added (excipients + drug), being an important indicator of suitability of a nano-scale delivery system (71).

3.2.3.1 Drug loading of DMF

Regarding the DMF loading within the nanoparticle, LCPS-7, LCPCS-8 and LCPS-9 were analyzed with HPLC methodology.

To prepare the samples for the characterization, 3 glasses of acetonitrile, each with the respective formulation were prepared with 9.9 mL of the solvent. 100 µL of the formulation was diluted in 9.9 mL of acetonitrile with a 0.01 dilution factor. Next, sonication at 35 Hz for 5 min took place to enhance the solubilization of the sample into the solvent. Finally, a quartz cuvette was filled with the preparation and analyzed three times at room temperature.

The analysis time was 4 min per sample. Peak heights rather than areas in the chromatography were recorded and measured at 210 nm. Concentrations of analyte were calculated by standard curves interpolation data recorded and DMF was quantified by HPLC (UV) Shimadzu Laboratory World, Tokyo, Japan) at $\lambda=358$ nm. This standard curve was used to convert the measured absorbance value into DMF concentration, which was then used for drug loading calculation using the following equation:

$$\% DL = \frac{\text{Amount of DMF loaded in the NP}}{\text{Total weight of the NP}} \times 100 \quad \text{Eq 1}$$

The linearity of the response was verified over the 0.2–50 µg/mL concentration range ($R^2>0.99$).

3.2.3.2 Drug loading of Rutin

In the matter of the concentration of the encapsulated rutin within the nanoparticle, in LCPS-13 and LCPS-14, formulations that carry the bioflavonoid, UV/Visible scanning spectrophotometry (Shimadzu UV-1800 UV/Visible Scanning Spectrophotometer) method was utilized at room temperature.

This method is the simplest technique to analyze bioflavonoids and the wavelength (λ) chosen for rutin was 359 nm as Abualhasan *et al* observed that in the UV-Visible this is the λ_{\max} in which rutin absorbs the most due to the conjugated double bonds with the aromatic groups. Such phenomenon occurs in this wavelength without interference of the excipients (72).

To prepare the samples, 3 glasses of dimethyl sulfoxide, DMSO, an organic and aprotic solvent was utilized to dilute the formulations. 100 μ L of the formulation was diluted in 9.9 mL of DMSO with a 0.01 dilution factor. Next, sonication at 35 Hz for 2 min at room temperature took place to enhance the solubilization of the sample into the solvent. Finally, a quartz cuvette was filled with the preparation and analyzed three times with the auto-zero executed in the first place. The following equation was used to determine the total drug loading of Rutin.

$$\% DL = \frac{\text{Amount of Rutin loaded in the NP}}{\text{Total weight of the NP}} \times 100 \quad \text{Eq 2}$$

4 Results and Discussion

4.1 Particle size and Polydispersity Index

4.1.1 Modified Nanoprecipitation: Sonication

The first two formulations, LCPS-1 and LCPS-2 were obtained only with the resource of the sonicator and the average diameter and size distribution of such samples are presented in Table 4.

The mean particle size and the size distribution represent the most essential parameters to describe the quality and stability of LPHNP. Such parameters are an important criterion of nanoparticles as these factors affect most of biological actions such as drug release rate, biodistribution, mucoadhesion, cellular uptake, where smaller size showed higher intracellular uptake than particles with larger size range (73).

As nanoparticles must go through an intranasal route, whether it be through the endocytic or extracellular path, the size and surface characteristics are an important criterion for the internalization. Thus, improving these parameters is important to enable an improvement of the cellular uptake into olfactory epithelial cells as well as the respiratory region cells (22).

The particle size of LCPS-1 reached 256 ± 1 nm while LCPCS-2 reached $600 \text{ nm} \pm 6$ nm and the polydispersity index ranged from 1.3 to 1.4 nm, respectively.

Regarding numerical value of PI ranges from 0.0 (for a perfectly uniform sample with respect to the particle size) to 1.0 (for a highly polydisperse sample with multiple particle size populations) (74). As both samples have a PI higher than 1, it means they are not homogeneous but heterogeneous which can alter the final product and performance of the formulations (74).

The first formulation was obtained with the Poloxamer F407 functioning as a surfactant however the second sample had Tween 80 as the excipient with the same function. The stirring time and speed remained the same in both formulations; therefore, conclusions regarding changes in these parameters may not be substantiated.

The hydrophilicity-lipophilicity balance of such stabilizer is an important concept in the choosing of the adequate surfactant in the colloidal system for its stability (75).

According to Prista, we must take into account the HLB values of either the dispersion and the potential surfactants. Thus, the most suitable choice would be the one with the closest value of the dispersion as it is the one who will increase the stability at its highest. Poloxamer F407 presents a 22 HLB, making a hydrophilic excipient associated with a very stable dispersion (59). On the other hand, Tween 80 presents a HLB of 15, which is lower, resulting in a lower stability, hence the choice of the poloxamer 407 for the upcoming formulations (LCPS-3 to LCPS-15).

Another reason to justify the LCPS-1 nanoparticles being smaller in size than LCPS-2's is the fact that cholesterol can stabilize the vesicle and the phospholipid bilayer, having an inversely proportional relationship with the particle size: the higher the amount of cholesterol, the lower the nanoparticle size is as there is an increase of the bilayer stabilization (76).

Thus, LCPS- 1 had 3% of cholesterol whereas LCPS-2 was prepared with 2% of the molecule, which in terms of particle size such results are viable according to literature.

Additionally, PEA had a double increase of percentage in LCPS-2 regarding LCPS-1. This higher amount of PEA can also explain the superior size of the second sample over the first. The chosen lipidic component to formulate the referenced nanoparticles is different: LCPS-1 contains lipoid-PEG 2000 while LCPS-2 contains PC, both in a 4% quantity. The impact of lipoid-PEG and PC will be further explained in the 4.1.4 Stability over time section.

Besides the excipients, the methodology and the preparation method of the nanoparticles also have an enormous role in the particle diameter and size distribution: Although the modified nanoprecipitation with the sonication is a rapid in reaction process, quick and non-toxic technique, it can help obtain small particles due to the high energy input, possibly resulting in an instability of the NP (77).

Taking these factors into account, we can draw the conclusion that between Tween 80 and Poloxamer F407, the latter is a more suitable stabilizer for the NP preparation. Additionally, the modified nanoprecipitation with the resource of the syringe pump may be a much more viable methodology to prepare them.

Therefore, the upcoming formulations will incorporate Poloxamer F407 as a stabilizer and exclusively prepared with the syringe pump technique.

Table 4: Mean diameter and mean polydispersity Index size of nanoparticles prepared by modified nanoprecipitation: sonication.

Formulation code	Particle Size \pm SD (nm)	Polidispersity Index Size \pm SD
LCPS-1	256 \pm 1	1.3 \pm 0
LCPS-2	600 \pm 6	1.4 \pm 0

SD: Standard deviation

4.1.3 Modified Nanoprecipitation: Syringe Pump Method

LCPS-3 to LCPS-15 were prepared with the syringe pump method and followed by solvent evaporation. Results of the particle size and polydispersity index on initial day of the analysis of each formulation is detailed in Table 5.

All formulations represented a model to understand how the different percentages of the excipients impacts the nanoparticles' physicochemical properties with and without the API. The percentage of PEA remained constant (2%) in all 12 formulations thus it is the correlation between the other diverse quantities and excipients we must consider.

With respect to the particle diameter and size distribution, the range of the results begins at 94 nm and ends at 341 nm whereas the PI ranges from 0.25 to 1.36.

The formulation with the smallest size was LCPS-11 that comprehended 94 nm and a PI of 0.29. This sample were the negative control of the hyaluronic acid and a hypothesis for these results will be further displayed in the 4.1.4 section regarding stability over time.

In contrast, LCPS-7 and LCPS-4 yielded the largest result at 341 nm. These formulations were not subjected to stability analysis as the initial result already exceeded the 300-nanometer limit for intranasal pathway.

As the remaining formulations were within the 300 nm limit, a progressive stability analysis was done to better evaluate the physicochemical characterization of the NP.

Table 5: Mean diameter and mean polydispersity Index size of nanoparticles prepared by modified nanoprecipitation: syringe pump technique.

Formulation code	Particle Size \pm SD (nm)	Polidispersity Index Size \pm SD
LCPS-3	187 \pm 3	1.19 \pm 0.04
LCPS-4	341 \pm 3	1.35 \pm 0.02
LCPS-5	229 \pm 4	1.10 \pm 0.02
LCPS-6	268 \pm 1	1.30 \pm 0.02
LCPS-7	341 \pm 17	1.36 \pm 0.01
LCPS-8	119 \pm 1	0.25 \pm 0.02
LCPS-9	244 \pm 4	1.24 \pm 0.02
LCPS-10	268 \pm 1	1.08 \pm 0
LCPS-11	94 \pm 0	0.29 \pm 0.01
LCPS-13	247 \pm 1	0.80 \pm 0.01
LCPS-14	256 \pm 15	1.25 \pm 0.02
LCPS-15	274 \pm 2	1.27 \pm 0.01

4.1.4 Stability over time

One of the parameters to assess the stability of the samples was by physicochemical characteristics.

Regarding LCPS-1, the results are shown in figure 10. On the second day of the analysis, the particle size had an increase over time of 4,3% and on the third day a 40% increase was shown as it reached 360 nm. The PI ranged from 1,3 on the first day of the analysis to 1,24 and 1,34 on the respective days, meaning that although throughout the time the formulation increased in diameter its distribution size remained constantly heterogeneous.

An important approach to improve the colloidal stability of LPHNP is the incorporation of suitable amounts of additional surfactants along with the phospholipids. For this reason, adding Poloxamer F407 (an amphiphilic biocompatible, biodegradable surfactant) along with PC confers stability of the NP (44).

As previously explained, LCPS-2 produced very large particles which are not to be considered. However, on the second day there was only a 10% decrease in size that is not significantly relevant. The superior size and its distribution can also be explained due to the solvent evaporation: if not well proceeded or not being done in enough time, monomer aggregation could increase the size of the samples. An optimal solvent:non-solvent ratio could also be optimized and produce an efficient process.

With these results, either the first and the second formulation reached values superior to the 300 nm limit, which is not in line with the intranasal route. Thus, this fact opens an ample room to optimize the critical process parameters for the development of these nanoparticles.

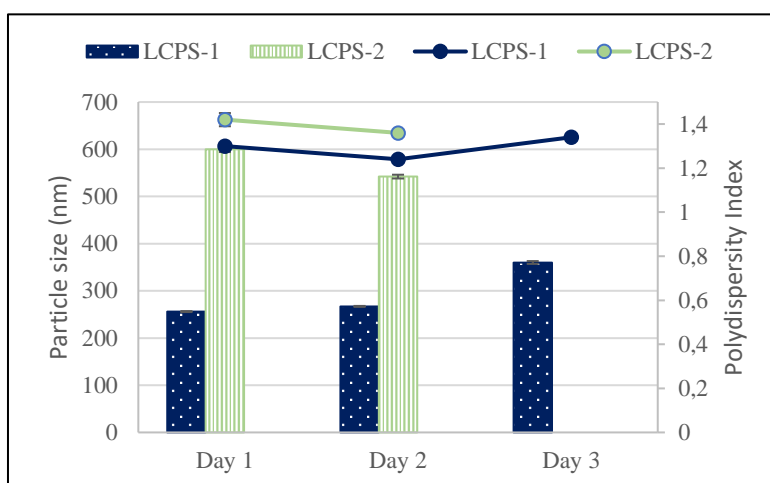


Figure 10: Physicochemical stability of LCPS-1 and LCPS-2, both formulations done with the resource of the sonicator.

Lipoid-PEG 2000 and phosphatidylcholine impact

LCPS-5 and LCPS-6 are composed of different lipidic components and figure 11 illustrates their physicochemical stability. LCPS-5 utilizes lipoid-PEG 2000, while LCPS-6 contains phosphatidylcholine as the lipidic component. Interestingly, both formulations maintain the same quantity of cholesterol and Poloxamer F407 in their compositions.

In the case of PC-kernel nanoparticles, there is a trend towards reducing their particle size while causing a slight increase in the polydispersity index (PI). Conversely, the Lipoid-PEG 2000 formulation appears to exhibit the opposite behavior, slightly increasing particle size while decreasing the PI.

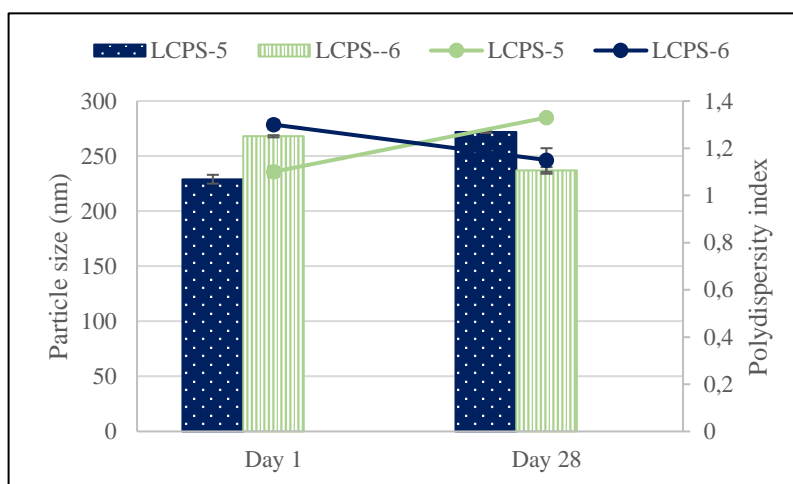


Figure 11: Physicochemical stability of LCPS-5 and LCPS-6, made with the resource of the syringe pump method.

Poloxamer impact on particle size and PI

Figure 12 illustrates the physicochemical stability of three different formulations: LCPS-3, LCPS-8, and LCPS-11. These formulations consistently maintained a particle size below 200 nanometers while exhibiting a polydispersity index ranging from 0.29 to 1.29. All three formulations contain the same quantity of the organic phase component Poloxamer F407. However, LCPS-3 stands out as the only formulation lacking this excipient in the aqueous phase. Consequently, the particle size of LCPS-3 is slightly larger compared to the other two formulations, suggesting that the inclusion of this co-polymer in the aqueous phase may contribute to reducing

particle size. On the other hand, LCPS-11 and LCPS-8 are also distinct as they do not contain hyaluronic acid, which may also account for its smaller particle size. The distinctive feature among them is the lipidic-core: LCPS-8 has PEGylated lipid, and LCPS-11 has PC, hence the inferior size of this last formulation. Nonetheless, analysis on this formulation must be done to infer the stability of these formulation and smaller/equal size nanoparticles should be expected. It's important to notice these results may also be influenced by the higher cholesterol amount although they have the same percentage.

LCPS-9 does not contain Poloxamer F407 on the organic phase nor the aqueous phase. Therefore, in figure 14 are displayed the results of this formulation. On the 15th day of analysis, 458 nm and a near 1,4 PI were reached, suggesting the absence of Poloxamer F407 has a big impact on the nanoparticle size and stability as it increases significantly. This formulation also has the biggest percentage of lipid-PEG 2000 (around 6%), therefore this excessive amount of excipient was able to exceed the particle size to the double.

In Figure 12 and 14, LCPS-3 and LCPS-10 are compared, both having identical amounts of various excipients. The key distinguishing factor between the two is the presence of Poloxamer F407: LCPS-10 includes this excipient in the aqueous phase, whereas LCPS-3 does not, leading to a larger particle size in LCPS-3 compared to the sample with Poloxamer F407 in the aqueous phase. These results might appear contradictory because, in other formulations, the absence of Poloxamer F407 tends to result in an increase in particle size rather than the decrease observed in this particular case. Therefore, more studies and analysis should be done to assess the parameters impacting these results.

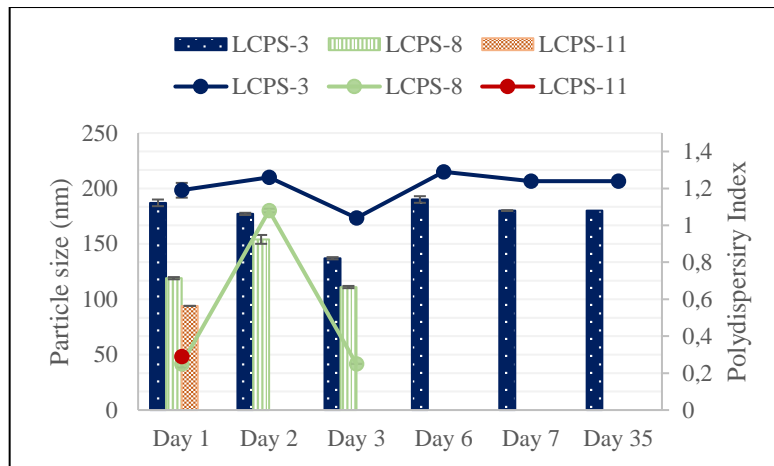


Figure 12: Physicochemical stability of LCPS-3, LCPS-8 and LCPS-11 made with the resource of the syringe pump.

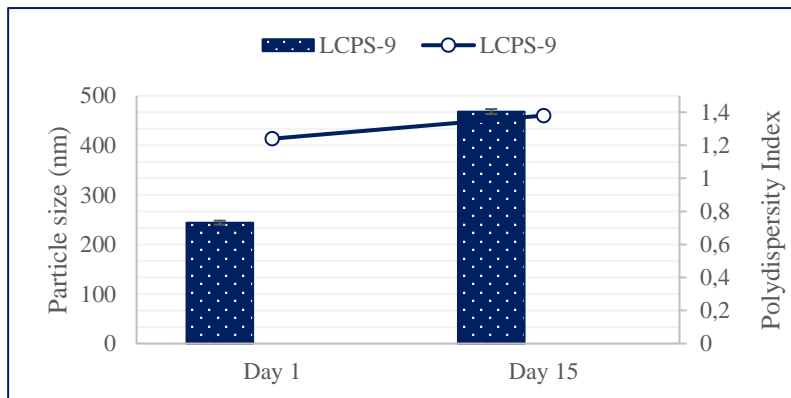


Figure 13: Physicochemical stability of LCPS-9 made with the resource of the syringe pump technique.

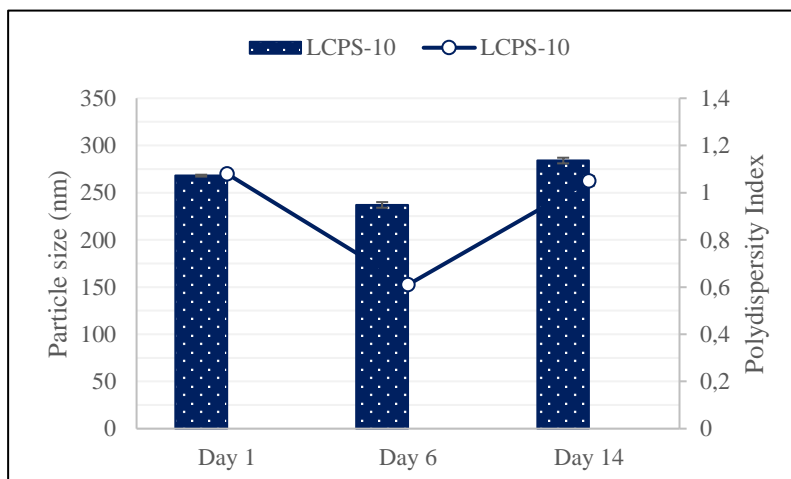


Figure 14: Physicochemical stability of LCPS-10 made with the resource of the syringe pump technique.

Non-HA-coated nanoparticles

For the negative control of HA, to formulation LCPS-8 and LCPS-11 this polysaccharide was not incorporated, and it is also important to convey they are the formulations with the smallest sizes (111 nm and 94 nm, respectively). Figure 15 represents these formulations' physicochemical stability.

The formulation with the smallest size was LCPS-11 that represented 94 nm and a PI of 0.29, making the particle size distribution homogeneous. Following closely was LCPS-8 with a particle size of 119 nm and a PI of 0.25. Both formulations did not incorporate HA but solely relied on Poloxamer in the water phase. One hypothesis to explain such observation is the compacted structure the absence of high-weight hyaluronic acid enables, reducing the spatial requirements. Thus, we can confirm the absence of HA as the polymeric shell can influence the nanoparticle size by reducing its size significantly. LCPS-14, illustrated in figure 16 does not contain hyaluronic acid as well however it does contain rutin, which can explain the biggest size.

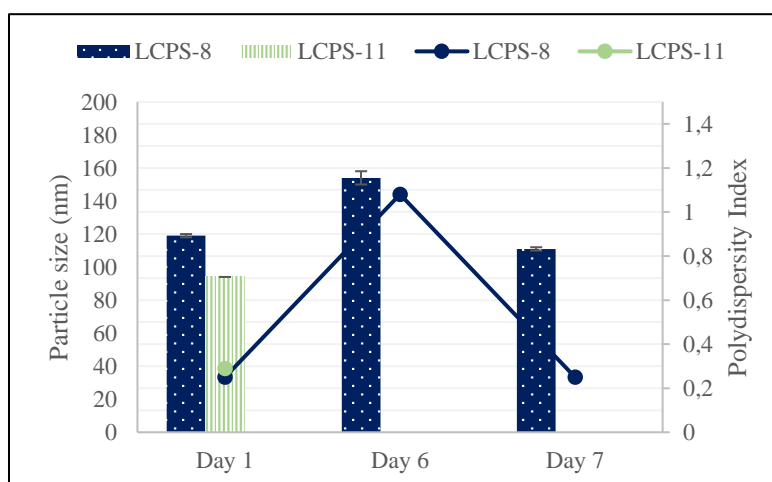


Figure 15: Physicochemical stability of LCPS-8 and LCPS-11 made with the resource of the syringe pump technique. These formulations do not contain HA.

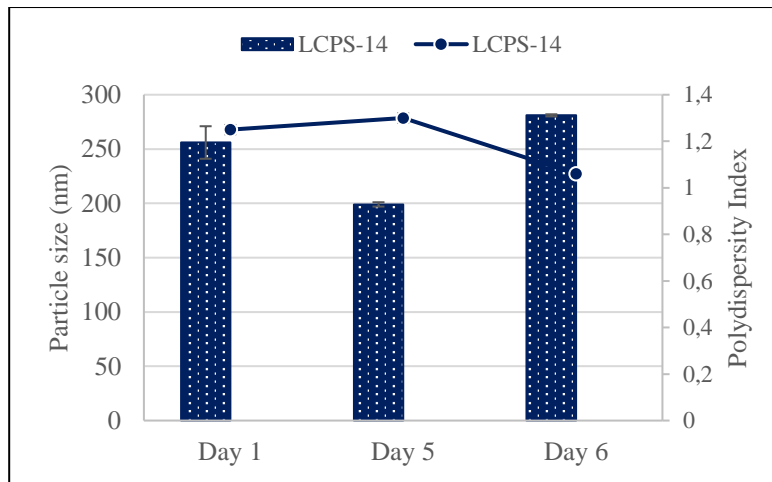


Figure 16: Physicochemical stability of LCPS-14 made with the resource of the syringe pump technique. This formulation does not contain HA.

DMF loaded nanoparticles

Regarding the formulations that indeed were incorporated DMF, LCPS-7, LCPS-8 and LCPS-15, their stability throughout time is shown in figure 17.

LCPS-7 attained 341 nm on the only day it got analyzed and a PI of 1,36 which makes the distribution of the particle size heterogeneous. The 2% cholesterol in such sample comparing to the 3% of cholesterol in LCPS-8 and LCPS-15 suggest the higher percentage of cholesterol enables a lower particle size. However, LCPS-15 reached 348 nm on the 7th day which does not enables for a concrete validation of such concept. This can be explained by the fact that even though the lipidic kernel is being stabilized by cholesterol and other components such as PEA, lipidic polymorphism and auto-oxidation may lead to its rearrangement and lower API incorporation, leading to an instability of the particle size (47). Moreover, this diameter exceeds the 300 nm upper limit which is not in accordance with the intranasal route criterion, reason why the drug loading was not assessed.

On the initial day of analysis, LCPS-8 achieved 119 nm and its size remained practically constant by the 6th and 7th day as the diameter reached 154 and 111 nm, respectively, showing a slight minimal change. The PI reached 0,25 in the last day of the analysis which suggests a homogeneous formulation even though it also reached 1,08 in the 6th day. These results can be explained not by a possible individual particle growth but by an increase of the agglomeration of the particles as the PI

increases along the diameter. An additional light microscopic analysis could be done to confirm this hypothesis. Poloxamer F407 and cholesterol percentages in LCPS-8 and LCPS-15 did not differ.

It's important to note that LCPS-8 did not contain HA, meaning that the absence of the natural polymer makes it practically a liposome as the polymeric component is lacking. The water phase only contains Poloxamer F407 and the lipidic component of this formulation is the lipid-PEG. Thus, such polymer enhances the steric stabilization of the nanoparticles that can also explain these results (34). Another important aspect lipid-PEG promotes is the ability to penetrate mucus and reduce the transmucosal movement of nanoparticles. However, this phenomenon is dependent on the molecular weight of the PEG-chain: the higher molecular weight, the more efficient it is in interacting with the mucus fibers (78). Lipid-PEG 2000 has very high chain value which enables a superior stability.

LCPS-15 got the range of values from 211 nm to 348 nm, and a PI ranging from 0,95 (on the second analysis day, which is a good indicator) however it reached values above 1 in the remaining days showing an inconsistent particle size distribution and consequently a fragile stability. Thus, as the diameter is superior to 300 nm, the intranasal pathway would not be the best route.

Hence, we can infer that LCPS-8 could be the most appropriate formulation to incorporate DMF in the light of particle size. As the polydispersity index decreased to values below 1, showcasing an homogeneous profile, and the diameter remains below 200, maintaining a good stability over time, this formulation is considered advantageous to be administered via the intranasal pathway. However, this formulation is lacking HA, so more studies need to be done with the aim of assessing the role HA would have if incorporated in this specific formulation.

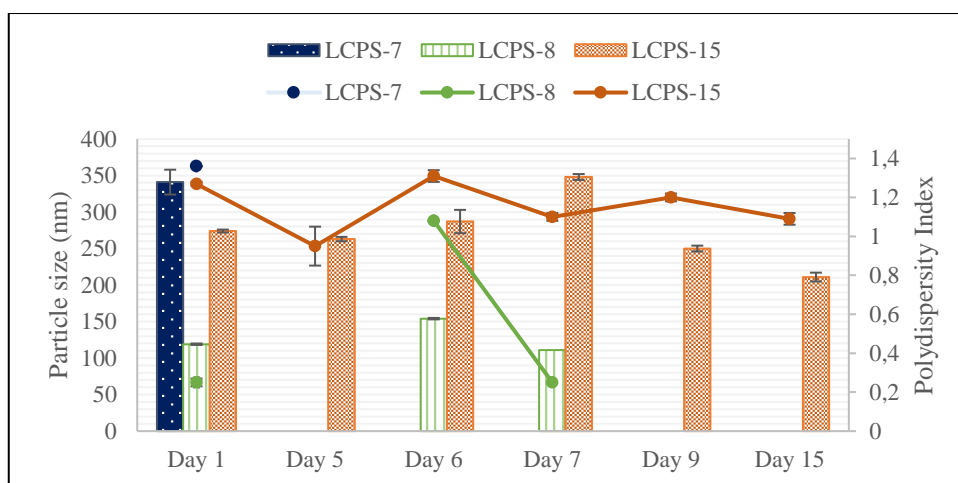


Figure 17: Physicochemical stability of LCPS-7, LCPS-8 and LCPS-15, made with the resource of the syringe pump. These formulations contain dimethyl fumarate.

Rutin-loaded nanoparticles

With the concern of nanoparticles containing rutin, the molecule is only entrapped within LCPS-13 and LCPS-14. Figure 18 represents its stability.

In the first formulation, the sizes underwent 247 nm and 270 nm with a PI of 0,8 in the first day, which is a good indicator of homogeneity but on the following days the same parameter exceeded 1.

Concerning LCPS-14, the particle diameter is inconsistent as it begins at 256 nm on the first day and becomes 199 nm and 281 nm on the second and third day, respectively. This formulation does not contain hyaluronic acid, therefore this feature opens an opportunity to further develop new studies showcasing the impact of HA in this specific formulation. The PI presented a heterogeneous distribution size as well as LCPS-13.

Either formulation could be convenient to carry rutin to be taken intranasally however their stability is not the best, hence an opportunity to do more research.

With the goal of decreasing the degradation of the phospholipids, lyophilization may have been a proper approach to promote a higher colloidal stability of LPHNP in storage (44).

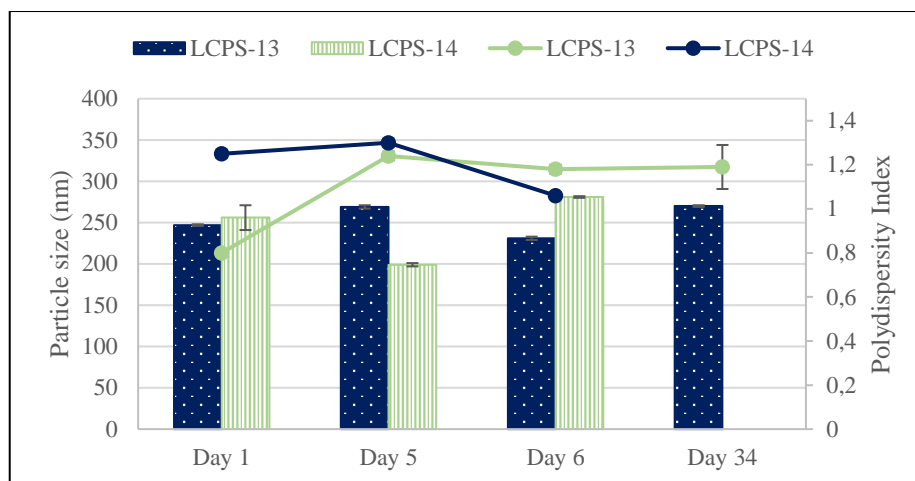


Figure 18: Physicochemical stability of LCPS-13 and LCPS-14 made with the resource of the syringe pump, both containing rutin.

Potential zeta

An important physicochemical parameter that was not assessed in this study but would help evaluate the nanoparticles behavior is the potential zeta. This factor characterizes the surface charge of the NP and comprehends the capacity nanoparticles have in aggregating with each other (79). The electric potential expected of a stable formulation is ± 30 mV as it demonstrates an electrostatic stability, whereas a minimum potential zeta of ± 20 mV indicates either an electrostatic and steric stability. This concept is important as the higher the potential zeta of a formulation is, the lower the aggregation of NP with each other occurs because of the increase of repulsion between the nanoparticles (80).

4.2 Drug Loading of the API

4.2.1. Drug loading of DMF

One of the most important parameters for defining polymer hybrid nanoparticles proposed to the drug loading range for any polymer or any excipient is the drug loading capacity (DL) (81).

Drug loading gives an idea about the amount of drug that is successfully entrapped/adsorbed into nanoparticles. Typically, an excellent drug carrier should have a high DL as it reduces the quantity of carrier to transport the required amount of API needs to the target site. This also helps reducing the drug wastage during the preparation of the NP.

Regarding DMF, the DL is 63% and 60% in LCPS-7 and LCPS-8, respectively, which is represented in table 6. These numbers are promising and a justification that is able to explain the results of both formulations is the lipidic polymorphism and re-arrangement as well as auto-oxidation in the lipidic core as it may lead to a DMF expulsion during long-term storage (47).

Differently from the physical stability that is an important concern for LPHNP, chemical stability is drug specific. As so, it can depend on the API solubility and the presence of certain functional groups: DMF contains an ester, making the molecule susceptible to hydrolytic degradation resulting in the drug loss (44).

Table 6: Drug loading of dimethyl fumarate within LCPS-7 and LCPS-8.

Formulation code	API	Drug loading (DL) %
LCPS-7	DMF	63±4
LCPS-8		60±6

4.2.2 Drug loading of Rutin

In regards of the formulations that contain rutin, table 7 represent the values from the drug loading represented in LCPS-13 and LCPS-14 and present promising results as the DL in both samples is higher than 70%, being 76% and 81% in LCPS-13 and LCPS-14, respectively. LCPS-13 is the most stable nanoparticle always reaching quite the same particle size and PI so we could infer this sample would be suitable for rutin's intranasal transport.

It is important to note that there are several factors that can influence the DL: aqueous solubility of the API, the affinity and the miscibility of it in the organic phase; the amount of the lipidic component, interactions between the lipid-API and the preparation method (40).

Table 7: Drug loading of dimethyl fumarate within LCPS-13 and LCPS-14.

Formulation code	API	Drug loading (DL) %
LCPS-13	Rutin	76±2
LCPS-14		81±4

5 Conclusion

Our research primarily focused on the development of 14 distinct hybrid nanoparticles with a projected lipidic-core and polymeric-shell. These nanoparticles contained PC or lipid-PEG 2000 as the lipid kernel and hyaluronic acid as the polymer. Apart from these components, in such formulations, different quantities of cholesterol, Poloxamer F407 and palmitoylethanolamide were incorporated in different quantities. Regarding the active pharmaceutical ingredient, some samples contained dimethyl fumarate, pharmaceutical advantageous on multiple sclerosis, while other formulations contained rutin. Both molecules reduce the neuroinflammatory state.

The formulations were prepared with the modified nanoprecipitation method with the sonicator as well as the modified nanoprecipitation method with the resource of the syringe pump technique. Regarding the characterization, particle size and polydispersity index were determined, and their stability was monitored in different time periods. A drug loading experiment was also conducted and the entrapment efficacy of DMF and Rutin were assessed by HPLC and UV spectrometry, respectively.

Formulations that were made with the resource of the sonicator had particles on the range of 200-600 nm, a very high value, meaning it is not the most feasible method of production of the nanoparticles. When produced with the syringe pump method, the range was 94 nm to 468 nm, indicating it produced smaller but not optimal particles. Poloxamer F407, cholesterol and PEA have an important role in stabilizing the nanoparticles and choice of either the lipidic kernel and the polymeric shell made of HA has an impact on the particle size and size distribution of the nanoparticle as well as its stability and further studies need to be done to better understand these results.

While the drug loading confers promising values of DMF and rutin there is still room to optimize the development of these hybrid nanoparticles. In terms of drug adsorption/encapsulation, transmission microscopic analysis should be done to visualize the nanoparticle morphology. Other techniques must be done to better assess the formulations' behavior regarding pharmacokinetics, such as: *in vitro* uptake of the formulations as well as *in vivo* uptake. These methods would help to better understand the further impact physicochemical characterization has on the intranasal delivery of nanoparticles as well as the best route to pursue.

6 References

1. Kumar P, Sharma G, Kumar R, Malik R, Singh B, Katare OP, et al. Enhanced Brain Delivery of Dimethyl Fumarate Employing Tocopherol-Acetate-Based Nanolipidic Carriers: Evidence from Pharmacokinetic, Biodistribution, and Cellular Uptake Studies. *ACS Chem Neurosci*. 2017 Apr 19;8(4):860–5.
2. Blair HA. Dimethyl Fumarate: A Review in Relapsing-Remitting MS. Vol. 79, *Drugs*. Adis; 2019. p. 1965–76.
3. Thompson AJ, Baneke P. Multiple Sclerosis International Federation (MSIF) Design and editorial support by Summers Editorial & Design Graphics by Nutmeg Productions Printed by Modern Colour Solutions [Internet]. 2013. Available from: www.msif.org
4. Doshi A, Chataway J. CMJv16n6S-Doshi.indd. Vol. 16, *Clinical Medicine*. 2016.
5. Burness CB, Deeks ED. Dimethyl fumarate: A review of its use in patients with relapsing-remitting multiple sclerosis. Vol. 28, *CNS Drugs*. Springer International Publishing; 2014. p. 373–87.
6. Dobson R, Giovannoni G. Multiple sclerosis – a review. Vol. 26, *European Journal of Neurology*. Blackwell Publishing Ltd; 2019. p. 27–40.
7. Patsopoulos NA, Barcellos LF, Hintzen RQ, Schaefer C, van Duijn CM, Noble JA, et al. Fine-Mapping the Genetic Association of the Major Histocompatibility Complex in Multiple Sclerosis: HLA and Non-HLA Effects. *PLoS Genet*. 2013 Nov 1;9(11).
8. Haines JL, Terwedow HA, Burgess K, Pericak-Vance MA, Rimmler JB, Martin ER, et al. Linkage of the MHC to familial multiple sclerosis suggests genetic heterogeneity The Multiple Sclerosis Genetics Group. Vol. 7, *Human Molecular Genetics*. 1998.
9. Cotsapas C, Mitrovic M, Hafler D. Multiple sclerosis. In 2018. p. 723–30.
10. Ríó J, Comabella M, Montalban X. Multiple sclerosis: Current treatment algorithms. *Curr Opin Neurol*. 2011 Jun;24(3):230–7.

11. Kim W, Zandoná ME, Kim SH, Kim HJ. Oral disease-modifying therapies for multiple sclerosis. *Journal of Clinical Neurology (Korea)*. 2015;11(1):9–19.
12. CHMP. Corr. 1 Committee for Medicinal Products for Human Use (CHMP) Assessment report Tecfidera [Internet]. 2013. Available from: www.ema.europa.eu
13. CHMP. Committee for Medicinal Products for Human Use (CHMP) Assessment report [Internet]. Available from: www.ema.europa.eu/contact
14. Maleki SJ, Crespo JF, Cabanillas B. Anti-inflammatory effects of flavonoids. *Food Chem*. 2019 Nov;299:125124.
15. Solanki I, Parihar P, Mansuri ML, Parihar MS. Flavonoid-based therapies in the early management of neurodegenerative diseases. Vol. 6, *Advances in Nutrition*. American Society for Nutrition; 2015. p. 64–72.
16. Ahmad N, Ahmad R, Naqvi AA, Alam MA, Ashafaq M, Samim M, et al. Rutin-encapsulated chitosan nanoparticles targeted to the brain in the treatment of Cerebral Ischemia. *Int J Biol Macromol*. 2016 Oct 1;91:640–55.
17. Habtemariam S, Varghese GK. Extractability of rutin in herbal tea preparations of moringa stenopetala leaves. *Beverages*. 2015 Sep 1;1(3):169–82.
18. Zlokovic B V. Blood-Brain Barrier and Neurovascular Mechanisms of Neurodegeneration and Injury Neurovascular System-Functional Hierarchy.
19. Mauludin R, Müller RH. Preparation and storage stability of rutin nanosuspensions. *J Pharm Investig*. 2013 Oct 24;43(5):395–404.
20. Wu D, Chen Q, Chen X, Han F, Chen Z, Wang Y. The blood–brain barrier: structure, regulation, and drug delivery. Vol. 8, *Signal Transduction and Targeted Therapy*. Springer Nature; 2023.
21. Bonferoni MC, Rossi S, Sandri G, Ferrari F, Gavini E, Rassa G, et al. Nanoemulsions for “nose-to-brain” drug delivery. *Pharmaceutics*. 2019 Feb 1;11(2).
22. Mistry A, Stolnik S, Illum L. Nanoparticles for direct nose-to-brain delivery of drugs. Vol. 379, *International Journal of Pharmaceutics*. 2009. p. 146–57.

23. Pires PC, Rodrigues M, Alves G, Santos AO. Strategies to Improve Drug Strength in Nasal Preparations for Brain Delivery of Low Aqueous Solubility Drugs. Vol. 14, *Pharmaceutics*. MDPI; 2022.
24. Battaglia L, Panciani PP, Muntoni E, Capucchio MT, Biasibetti E, De Bonis P, et al. Lipid nanoparticles for intranasal administration: application to nose-to-brain delivery. Vol. 15, *Expert Opinion on Drug Delivery*. Taylor and Francis Ltd; 2018. p. 369–78.
25. Daneman R, Prat A. The blood–brain barrier. *Cold Spring Harb Perspect Biol*. 2015 Jan 1;7(1).
26. Trevino JT, Quispe RC, Khan F, Novak V. Non-Invasive Strategies for Nose-to-Brain Drug Delivery.
27. Gänger S, Schindowski K. Tailoring formulations for intranasal nose-to-brain delivery: A review on architecture, physico-chemical characteristics and mucociliary clearance of the nasal olfactory mucosa. Vol. 10, *Pharmaceutics*. MDPI AG; 2018.
28. Bonferoni MC, Rassa G, Gavini E, Sorrenti M, Catenacci L, Giunchedi P. Nose-to-brain delivery of antioxidants as a potential tool for the therapy of neurological diseases. *Pharmaceutics*. 2020 Dec 1;12(12):1–21.
29. Jeong SH, Jang JH, Lee YB. Drug delivery to the brain via the nasal route of administration: exploration of key targets and major consideration factors. *J Pharm Investig*. 2023 Jan 24;53(1):119–52.
30. Lockman PR, Mumper RJ, Khan MA, Allen DD. Nanoparticle Technology for Drug Delivery Across the Blood-Brain Barrier [Internet]. Vol. 28, *Drug Development and Industrial Pharmacy*. 2002. Available from: www.dekker.com
31. Mauludin R, Müller RH. Preparation and storage stability of rutin nanosuspensions. *J Pharm Investig*. 2013 Oct 24;43(5):395–404.
32. Mistry A, Glud SZ, Kjems J, Randel J, Howard KA, Stolnik S, et al. Effect of physicochemical properties on intranasal nanoparticle transit into murine olfactory epithelium. *J Drug Target*. 2009 Aug;17(7):543–52.

33. Alberto M, Paiva-Santos AC, Veiga F, Pires PC. Lipid and Polymeric Nanoparticles: Successful Strategies for Nose-to-Brain Drug Delivery in the Treatment of Depression and Anxiety Disorders. Vol. 14, *Pharmaceutics*. MDPI; 2022.
34. Pardeshi C V., Belgamwar VS, Tekade AR, Surana SJ. Novel surface modified polymer-lipid hybrid nanoparticles as intranasal carriers for ropinirole hydrochloride: In vitro, ex vivo and in vivo pharmacodynamic evaluation. *J Mater Sci Mater Med*. 2013 Sep;24(9):2101–15.
35. Beija M, Salvayre R, Lauth-de Viguerie N, Marty JD. Colloidal systems for drug delivery: From design to therapy. Vol. 30, *Trends in Biotechnology*. 2012. p. 485–96.
36. Garg T, Rath G, Goyal AK. Colloidal Drug Delivery Systems: Current Status and Future Directions [Internet]. Vol. 32, *Critical Reviews™ in Therapeutic Drug Carrier Systems*. 2015. Available from: www.begellhouse.com
37. Najahi-Missaoui W, Arnold RD, Cummings BS. Safe nanoparticles: Are we there yet? *Int J Mol Sci*. 2021 Jan 1;22(1):1–22.
38. Mukherjee A, Waters AK, Kalyan P, Achrol AS, Kesari S, Yenugonda VM. Lipid-polymer hybrid nanoparticles as a nextgeneration drug delivery platform: State of the art, emerging technologies, and perspectives. Vol. 14, *International Journal of Nanomedicine*. Dove Medical Press Ltd.; 2019. p. 1937–52.
39. Sivadasan D, Sultan MH, Madkhali O, Almoshari Y, Thangavel N. Polymeric lipid hybrid nanoparticles (Plns) as emerging drug delivery platform—a comprehensive review of their properties, preparation methods, and therapeutic applications. Vol. 13, *Pharmaceutics*. MDPI; 2021.
40. Sivadasan D, Sultan MH, Madkhali O, Almoshari Y, Thangavel N. Polymeric lipid hybrid nanoparticles (Plns) as emerging drug delivery platform—a comprehensive review of their properties, preparation methods, and therapeutic applications. Vol. 13, *Pharmaceutics*. MDPI; 2021.
41. Govender S, Lutchman D, Pillay V, Chetty DJ, Govender T. Enhancing drug incorporation into tetracycline-loaded chitosan microspheres for periodontal therapy. *J Microencapsul*. 2006 Nov;23(7):750–61.

42. Hadinoto K, Sundaresan A, Cheow WS. Lipid-polymer hybrid nanoparticles as a new generation therapeutic delivery platform: A review. Vol. 85, *European Journal of Pharmaceutics and Biopharmaceutics*. Elsevier B.V.; 2013. p. 427–43.
43. Lockman PR, Mumper RJ, Khan MA, Allen DD. Nanoparticle Technology for Drug Delivery Across the Blood-Brain Barrier [Internet]. Vol. 28, *Drug Development and Industrial Pharmacy*. 2002. Available from: www.dekker.com
44. Mandal B, Bhattacharjee H, Mittal N, Sah H, Balabathula P, Thoma LA, et al. Core-shell-type lipid-polymer hybrid nanoparticles as a drug delivery platform. *Nanomedicine*. 2013 May;9(4):474–91.
45. Pardeshi C V., Belgamwar VS, Tekade AR, Surana SJ. Novel surface modified polymer-lipid hybrid nanoparticles as intranasal carriers for ropinirole hydrochloride: In vitro, ex vivo and in vivo pharmacodynamic evaluation. *J Mater Sci Mater Med*. 2013 Sep;24(9):2101–15.
46. Kaczmarek JC, Patel AK, Kauffman KJ, Fenton OS, Webber MJ, Heartlein MW, et al. Polymer-Lipid Nanoparticles for Systemic Delivery of mRNA to the Lungs. *Angewandte Chemie - International Edition*. 2016 Oct 24;55(44):13808–12.
47. Zhang RX, Ahmed T, Li LY, Li J, Abbasi AZ, Wu XY. Design of nanocarriers for nanoscale drug delivery to enhance cancer treatment using hybrid polymer and lipid building blocks. Vol. 9, *Nanoscale*. Royal Society of Chemistry; 2017. p. 1334–55.
48. Maurya P, Singh S, Saraf SA. Inhalable hybrid nanocarriers for respiratory disorders. In: *Targeting Chronic Inflammatory Lung Diseases Using Advanced Drug Delivery Systems*. Elsevier; 2020. p. 281–302.
49. ZHANG L, ZHANG L. LIPID-POLYMER HYBRID NANOPARTICLES: SYNTHESIS, CHARACTERIZATION AND APPLICATIONS. *Nano Life*. 2010 Mar;01(01n02):163–73.

50. Bilati U, Allémann E, Doelker E. Development of a nanoprecipitation method intended for the entrapment of hydrophilic drugs into nanoparticles. *European Journal of Pharmaceutical Sciences*. 2005 Jan;24(1):67–75.
51. Fessi H, Puisieux F, Devissaguet JPh, Ammoury N, Benita S. Nanocapsule formation by interfacial polymer deposition following solvent displacement. *Int J Pharm*. 1989 Oct;55(1):R1–4.
52. Shah S, Famta P, Raghuvanshi RS, Singh SB, Srivastava S. Lipid polymer hybrid nanocarriers: Insights into synthesis aspects, characterization, release mechanisms, surface functionalization and potential implications. Vol. 46, *Colloids and Interface Science Communications*. Elsevier B.V.; 2022.
53. Jelvehgari M, Salatin S, Barar J, Barzegar-Jalali M, Adibkia K, Kiafar F, et al. Development of a nanoprecipitation method for the entrapment of a very water soluble drug into Eudragit RL nanoparticles. Vol. 12, *Research in Pharmaceutical Sciences*. 2017.
54. Rietscher R, Thum C, Lehr CM, Schneider M. Semi-Automated Nanoprecipitation-System—An Option for Operator Independent, Scalable and Size Adjustable Nanoparticle Synthesis. *Pharm Res*. 2015 Jun 30;32(6):1859–63.
55. Mallick S, Thuy LT, Lee S, Park JI, Choi JS. Liposomes containing cholesterol and mitochondria-penetrating peptide (MPP) for targeted delivery of antimycin A to A549 cells. *Colloids Surf B Biointerfaces*. 2018 Jan;161:356–64.
56. Ruwizhi N, Aderibigbe BA. The efficacy of cholesterol-based carriers in drug delivery. Vol. 25, *Molecules*. MDPI AG; 2020.
57. Menon JU, Kona S, Wadajkar AS, Desai F, Vadla A, Nguyen KT. Effects of surfactants on the properties of PLGA nanoparticles. *J Biomed Mater Res A*. 2012;100 A(8):1998–2005.
58. Zaman M, Iqbal A, Sarwar HS, Butt MH, Iqbal MO, Nissar N, et al. Application of Nanoprecipitation Technique to Develop Poloxamer-407 Facilitated Solid Lipid Nanoparticles for the Controlled Delivery of Tacrolimus. *Int J Polym Sci*. 2023;2023.

59. Dumortier G, Grossiord JL, Agnely F, Chaumeil JC. A review of poloxamer 407 pharmaceutical and pharmacological characteristics. Vol. 23, *Pharmaceutical Research*. Springer Science and Business Media Deutschland GmbH; 2006. p. 2709–28.
60. Moghimi SM, Hunter AC, Moghimi SM, Hunter AC, Murray JC. Long-Circulating and Target-Specific Nanoparticles: Theory to Practice The imbalance of Follistatin and ActivinA during the genesis of lung adenocarcinoma View project Long-Circulating and Target-Specific Nanoparticles: Theory to Practice [Internet]. 2001. Available from: <http://pharmrev.aspetjournals.org>
61. Clayton P, Hill M, Bogoda N, Subah S, Venkatesh R. Palmitoylethanolamide: A Natural Compound for Health Management. *Int J Mol Sci*. 2021 May 18;22(10):5305.
62. Puglia C, Blasi P, Ostacolo C, Sommella E, Bucolo C, Platania CBM, et al. Innovative Nanoparticles Enhance N-Palmitoylethanolamide Intraocular Delivery. *Front Pharmacol*. 2018 Mar 28;9.
63. Tiwari S, Bahadur P. Modified hyaluronic acid based materials for biomedical applications. Vol. 121, *International Journal of Biological Macromolecules*. Elsevier B.V.; 2019. p. 556–71.
64. Rao NV, Rho JG, Um W, Ek PK, Nguyen VQ, Oh BH, et al. Hyaluronic acid nanoparticles as nanomedicine for treatment of inflammatory diseases. Vol. 12, *Pharmaceutics*. MDPI AG; 2020. p. 1–18.
65. Tian X, Azpurua J, Hine C, Vaidya A, Myakishev-Rempel M, Abulaeva J, et al. High-molecular-mass hyaluronan mediates the cancer resistance of the naked mole rat. *Nature*. 2013;499(7458):346–9.
66. Suksiriworapong J, Pongprasert N, Bunsupa S, Taresco V, Crucitti VC, Janurai T, et al. CD44-Targeted Lipid Polymer Hybrid Nanoparticles Enhance Anti-Breast Cancer Effect of Cordyceps militaris Extracts. *Pharmaceutics*. 2023 Jun 20;15(6):1771.

67. Maher R, Moreno-Borralló A, Jindal D, Mai BT, Ruiz-Hernandez E, Harkin A. Intranasal Polymeric and Lipid-Based Nanocarriers for CNS Drug Delivery. Vol. 15, *Pharmaceutics*. MDPI; 2023.
68. Curcio M, Cirillo G, Rouaen JRC, Saletta F, Nicoletta FP, Vittorio O, et al. Natural polysaccharide carriers in brain delivery: Challenge and perspective. Vol. 12, *Pharmaceutics*. MDPI AG; 2020. p. 1–26.
69. Samaridou E, Walgrave H, Salta E, Álvarez DM, Castro-López V, Loza M, et al. Nose-to-brain delivery of enveloped RNA - cell permeating peptide nanocomplexes for the treatment of neurodegenerative diseases. *Biomaterials*. 2020 Feb 1;230.
70. Model 100 Series User's Manual.
71. IEEE Engineering in Medicine and Biology Society. Annual International Conference (41st : 2019 : Berlin G, IEEE Engineering in Medicine and Biology Society, Institute of Electrical and Electronics Engineers. 2019 41st Annual International Conference of the IEEE Engineering in Medicine and Biology Society (EMBC) : Biomedical Engineering Ranging from Wellness to Intensive Care : 41st EMB Conference 2019 : July 23-27, Berlin.
72. Abualhasan MN, Mansour J, Jaradat N, Zaid AN, Khadra I. Formulation and Development of a Validated UV-Spectrophotometric Analytical Method of Rutin Tablet. *Int Sch Res Notices*. 2017 May 16;2017:1–7.
73. Hamishehkar H, Ghaderi S, Ghanbarzadeh S. Evaluation of Different Methods for Preparing Nanoparticle Containing Gammaoryzanol for Potential Use in Food Fortification [Internet]. Vol. 20, *Pharmaceutical Sciences*. 2015. Available from: <http://journals.tbzmed.ac.ir/PHARM>
74. Danaei M, Dehghankhold M, Ataei S, Hasanzadeh Davarani F, Javanmard R, Dokhani A, et al. Impact of particle size and polydispersity index on the clinical applications of lipidic nanocarrier systems. Vol. 10, *Pharmaceutics*. MDPI AG; 2018.
75. L. Nogueira Prista ACA e RM. *TECNOLOGIA FARMACÊUTICA* . 4th ed. Fundação Calouste Gulbenkian, editor. Vol. II volume. Lisboa; 1995.

76. Raeiszadeh M, Pardakhty A, Sharififar F, Mehrabani M, Nejat-Mehrab-Kermani E H, Mehrabani M. Phytoniosome: a Novel Drug Delivery for Myrtle Extract. *Iranian Journal of Pharmaceutical Research*. 2018.
77. Hernández-Giottonini KY, Rodríguez-Córdova RJ, Gutiérrez-Valenzuela CA, Peñuñuri-Miranda O, Zavala-Rivera P, Guerrero-Germán P, et al. PLGA nanoparticle preparations by emulsification and nanoprecipitation techniques: Effects of formulation parameters. Vol. 10, *RSC Advances*. Royal Society of Chemistry; 2020. p. 4218–31.
78. Huckaby JT, Lai SK. PEGylation for enhancing nanoparticle diffusion in mucus. Vol. 124, *Advanced Drug Delivery Reviews*. Elsevier B.V.; 2018. p. 125–39.
79. Singh R, Lillard JW. Nanoparticle-based targeted drug delivery. Vol. 86, *Experimental and Molecular Pathology*. 2009. p. 215–23.
80. Jelvehgari M, Salatin S, Barar J, Barzegar-Jalali M, Adibkia K, Kiafar F, et al. Development of a nanoprecipitation method for the entrapment of a very water soluble drug into Eudragit RL nanoparticles. Vol. 12, *Research in Pharmaceutical Sciences*. 2017.
81. Baghel YS, Bhattacharya S. Lipid Polymeric Hybrid Nanoparticles: Formulation Techniques and Effects on Glioblastoma. Vol. 28, *Pharmaceutical Sciences*. Tabriz University of Medical Sciences; 2022. p. 174–93.